

Sketched Ridgeless Linear Regression: The Role of Downsampling

Xin Chen^{*†} Yicheng Zeng^{*‡} Siyue Yang[§] Qiang Sun[§]

Abstract

Overparametrization often helps improve the generalization performance. This paper proposes a dual view of overparametrization suggesting that downsampling may also help generalize. Motivated by this dual view, we characterize two out-of-sample prediction risks of the sketched ridgeless least square estimator in the proportional regime $m \asymp n \asymp p$, where m is the sketching size, n the sample size, and p the feature dimensionality. Our results reveal the statistical role of downsampling. Specifically, downsampling does not always hurt the generalization performance, and may actually help improve it in some cases. We identify the optimal sketching sizes that minimize the out-of-sample prediction risks, and find that the optimally sketched estimator has stabler risk curves that eliminates the peaks of those for the full-sample estimator. We then propose a practical procedure to empirically identify the optimal sketching size. Finally, we extend our results to cover central limit theorems and misspecified models. Numerical studies strongly support our theory.

Keywords: Downsampling, minimum-norm solutions, overparametrization, random sketching, ridgeless least square estimators.

Contents

1	Introduction	3
1.1	Related work	5
2	Preliminaries	6
2.1	Sketching matrix	6
2.2	Out-of-sample prediction risk	7
2.3	Assumptions	8

^{*}The first two authors contributed equally.

[†]Department of Operations Research and Financial Engineering, Princeton University, 98 Charlton St, Princeton, NJ 08544, USA; E-mail: xc5557@princeton.edu.

[‡]Shenzhen Research Institute of Big Data, the Chinese University of Hong Kong, 2001 Longxiang Boulevard, Shenzhen, Guangdong, China; E-mail: statzyc@sribd.cn. Yicheng Zeng was a postdoctoral fellow at the University of Toronto when the bulk of this work was done.

[§]Department of Statistical Sciences, University of Toronto, 700 University Ave, Toronto, ON M5G 1X6, Canada; E-mail: syue.yang@mail.utoronto.ca, qiang.sun@utoronto.ca.

3 A warm-up case: Isotropic features	9
3.1 Limiting risks	9
3.2 Optimal sketching size	11
4 Correlated features	13
4.1 Overparameterized regime	13
4.2 Underparameterized regime	14
5 A practical procedure	15
6 Extensions	17
6.1 Deterministic β case	17
6.2 Central limit theorem	19
6.3 Misspecified model	21
7 Conclusions and Discussions	22
A Details on numerical studies	26
A.1 Numerical studies for isotropic features	26
A.1.1 Figure 2	26
A.1.2 Figure 3	26
A.2 Numerical studies for correlated features	27
A.2.1 Figure 4	27
A.2.2 Figure 5	27
B Proofs for isotropic features	28
B.1 Proof of Lemma 3.1	28
B.2 Proof of Theorem 3.2	28
B.3 Proof of Theorem 3.3	28
C Proofs for correlated features	29
C.1 Proofs for the over-parameterized case	29
C.1.1 Proof of Lemma 4.1	29
C.1.2 Proof of Theorem 4.2	29
C.2 Proofs for the under-parameterized case	35
C.2.1 Proof of Theorem 4.3	35
C.2.2 Proof of Corollary 4.4	36
C.2.3 Proof of Corollary 4.5	37
D Proof of Theorem 6.2	37

E Proofs for central limit theorems	40
E.1 Proof of Theorem 6.4	40
E.2 Proof of Theorem 6.5	41
E.3 Proof of Theorem 6.7	42

1 Introduction

According to international data corporation, worldwide data will grow to 175 zettabytes by 2025, with as much of the data residing in the cloud as in data centers. These data have potential to revolutionize operations and analytics, from engineering to science. The sizes of these data, however, have posed unprecedented computational challenges as many existing statistical methods and learning algorithms often prove ineffective for scaling to large datasets. In recent years, sketch-and-solve methods, also referred to as sketching algorithms, have proven to be powerful for approximate computations over large datasets (Pilanci, 2016; Mahoney, 2011). A sketching algorithm first constructs a small “sketch” of the full dataset by using random sketching/projection or random sampling methods, and then uses this sketched dataset as a surrogate to perform analyses of interest for the full dataset.

To fix the idea, we consider the linear regression problem. Suppose we have collected identically and independent distributed (i.i.d.) data according to

$$y_i = \beta^T x_i + \varepsilon_i, \quad i = 1, \dots, n, \quad (1.1)$$

where $y_i \in \mathbb{R}$ is the label of the i -th observation, $\beta \in \mathbb{R}^p$ is the unknown regression coefficient vector, $x_i \in \mathbb{R}^p \sim x \sim P_x$ is the p -dimensional feature vector of the i -th observation such that P_x is a probability law on \mathbb{R}^p with $\mathbb{E}(x) = 0$ and $\text{cov}(x) = \Sigma$, and $\varepsilon_i \sim \varepsilon \sim P_\varepsilon$ is the i -th random noise independent of x_i such that P_ε is a probability law on \mathbb{R} with $\mathbb{E}(\varepsilon) = 0$ and $\text{var}(\varepsilon) = \sigma^2$. In matrix form, we have $Y = X\beta + \varepsilon$, where $X = (x_1, \dots, x_n)^T \in \mathbb{R}^{n \times p}$, $Y = (y_1, \dots, y_n)^T \in \mathbb{R}^n$ and $\varepsilon = (\varepsilon_1, \dots, \varepsilon_n)^T \in \mathbb{R}^n$. We consider the following ridgeless least square estimator

$$\widehat{\beta} := (X^T X)^+ X^T Y = \lim_{\lambda \rightarrow 0^+} (X^T X + n\lambda I_p)^{-1} X^T Y,$$

where $(\cdot)^+$ denotes the Moore-Penrose pseudoinverse and $I_p \in \mathbb{R}^{p \times p}$ is the identity matrix. In the case of $\text{rank}(X) = p$, $\widehat{\beta}$ reduces to the ordinary least square (OLS) estimator, which is the de-facto standard for linear regression problems and has many optimality properties. Computing the OLS estimator, for instance via QR decomposition (Golub & Van Loan, 2013), has a computational complexity of $O(np^2)$, so the computation of the full-sample OLS estimator is prohibitive when the sample size n and dimensionality p are of millions or even billions.

Sketching algorithms alleviate the computational burden by reducing the data size. Specifically, sketching multiplies the full data (X, Y) by an $m \times n$ sketching matrix S to

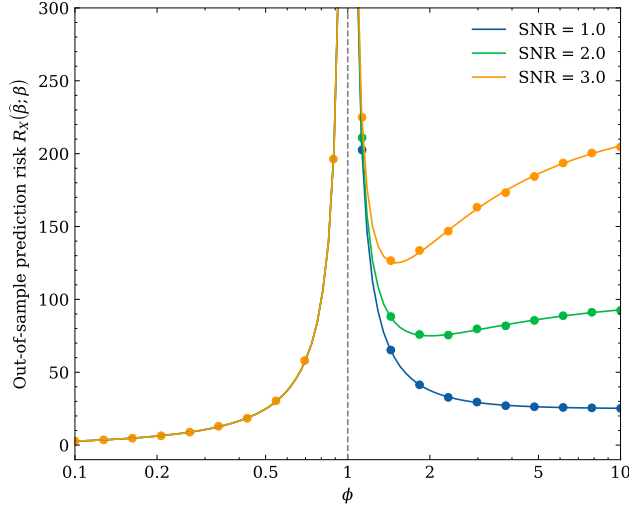


Figure 1: Asymptotic risk curves for the ridgeless least square estimator, as functions of $\phi = p/n$. The blue, green, and yellow lines are theoretical risk curves for SNR = $\alpha/\sigma = 1, 2, 3$ with (α, σ) taking $(5, 5)$, $(10, 5)$ and $(15, 5)$, respectively. The dots mark the finite-sample risks with $n = 400$, ϕ varying in $[0.1, 10]$ and $p = [n\phi]$. Each row of the feature matrix $X \in \mathbb{R}^{n \times p}$ was i.i.d. drawn from $\mathcal{N}(0, I_p)$.

obtain the sketched data $(SX, SY) \in \mathbb{R}^{m \times p} \times \mathbb{R}^m$, where we call $m < n$ the sketching size. Instead of computing the full-sample OLS estimator, we then compute the sketched ridgeless least square estimator based on the sketched data as

$$\widehat{\beta}^S = (X^T S^T S X)^+ X^T S^T S Y = \lim_{\lambda \rightarrow 0^+} (X^T S^T S X + n\lambda I_p)^{-1} X^T S^T S Y. \quad (1.2)$$

The total computational complexity for computing the sketched data and sketched least square estimator is on the order of $O(np \log m + mp^2)$ when using fast orthogonal sketches (Pilanci, 2016). The common belief is that sketching helps reduce the run-time complexity at the sacrifice of statistical accuracy (Woodruff, 2014; Raskutti & Mahoney, 2016; Drineas & Mahoney, 2018; Dobriban & Liu, 2018). Indeed, as Dobriban & Liu (2018) pointed out, a larger number of samples leads to a higher accuracy. They showed that, in the case of orthogonal sketches, if one sketches to m samples such that $p < m < n$, the test error increases by a factor of $m(n-p)/\{n(m-p)\} > 1$, which equals 1.1 when $m = 10^6$, $n = 10^7$, and $p = 10^5$. Raskutti & Mahoney (2016) reported a similar phenomenon by considering the regime $n \gg p$ and various error criteria. These results, however, only focus on the underparameterized regime, i.e. $p < n$, and do not reveal the statistical role of downsampling in a broader regime. We therefore ask the following questions:

What is the statistical role of downsampling? Does downsampling always hurt the statistical accuracy?

This paper answers the above questions in the case of sketched ridgeless least square estimators (1.2) in both underparameterized and overparameterized regimes where downsampling is realized by random sketching. Our intuition is that downsampling plays a

similar role as that of increasing the model capacity. Because increasing the model capacity has been recently observed in modern machine learning practice to often help improve the generalization performance (He et al., 2016; Neyshabur et al., 2014; Novak et al., 2018; Belkin et al., 2018), downsampling may also benefit generalization properties (Nakkiran et al., 2021). This “dual view” can be seen clearly in the case of linear regression, where the out-of-sample prediction risk only depends on the model size and sample size via the quantity p/n (Hastie et al., 2022); see Figure 1. Thus increasing the model size p has exactly the same effect as downsampling the sample size n .

Motivated by this dual view, we characterize two out-of-sample prediction risks of the sketched ridgeless least square estimator in the proportional regime $m \asymp n \asymp p$. The sketching matrices we considered are general sketching matrices that only need to satisfy some mild assumption, i.e., Assumption 2.6, and thus include many sketching matrices in the literature as special cases. Our concrete contributions are as follows. First, we provide asymptotically exact formulas of the two out-of-sample prediction risks in the proportional regime. This reveals the statistical role of downsampling in terms of the generalization performance. Perhaps surprisingly at first glance, we find that downsampling does not always hurt the generalization performance, and may actually help improve it in some cases. Second, we show that the orthogonal sketching is optimal among all types of sketching considered in the underparameterized case, which was also pointed out by Dobriban & Liu (2018). In the overparameterized case however, all general sketching matrices are equivalent to each other. Third, we identify the optimal sketching sizes that minimize the out-of-sample prediction risks. The optimally sketched ridgeless least square estimators exhibit universally better risk curves when varying the model size, and are thus stabler than the full-sample ones. Forth, we propose a practical procedure to empirically identify the optimal sketching size by using an additional validation dataset, which can be of a small size in our experiments. Fifth, in addition to the characterization on first-order limits, we also provide central limit theorems on the risks. Technically, by leveraging results on random matrix theory for covariance matrices (Zhang, 2007; El Karoui, 2009; Knowles & Yin, 2017; Zheng et al., 2015), we provide almost sure convergence results for the test risks while Dobriban & Liu (2018) studied the asymptotic limit of expected risks. Their results on out-of-sample prediction risk can be recovered from ours by using the dominated convergence theorem.

The rest of this paper proceeds as follows. We close this section with more related work. Section 2 gives some preliminaries. Section 3 studies the out-of-sample prediction risks under isotropic features while Section 4 is for correlated features. We provide a simple yet practical procedure to pick the best possible sketching size in Section 5. We extend our results in several directions in Section 6. Conclusions and discussions are collected in Section 7.

1.1 Related work

We review some related work that are closely related to ours.

Generalization properties of overparameterized models The generalization properties of over-parametrized models have been widely studied in recently years. It starts with the observation that overparameterized neural networks often achieve benign generalization performance, even when the networks are trained without any explicit regularization (He et al., 2016; Neyshabur et al., 2014; Cenzianni et al., 2016; Novak et al., 2018; Zhang et al., 2021; Bartlett et al., 2020; Liang & Rakhlin, 2020). Belkin et al. (2018) furthered this line of studies by positing the “double descent” performance curve for models beyond neural networks. The double descent curve subsumes the textbook U-shape bias-variance-tradeoff curve (Hastie et al., 2009) by showing how increasing model capacity beyond certain interpolation threshold results in improved test errors. Follow-up papers aim to characterize this double descent phenomenon for various simplified models, including the linear model (Hastie et al., 2022; Richards et al., 2021), the random feature model (Mei & Montanari, 2022) and the partially optimized two-layer neural network (Ba et al., 2019), among others.

Implicit regularization and minimum ℓ_2 -norm solutions Another line of research focuses on explaining benign overfitting via implicit regularization of overparameterized models (Neyshabur et al., 2014). For example, Gunasekar et al. (2018) and Zhang et al. (2021) showed that gradient descent (GD) converges to the minimum ℓ_2 -norm solutions for linear regression problems, which are exactly the ridgeless least squares estimators. Hastie et al. (2022) characterized the exact out-of-sample prediction risk for the ridgeless least square estimator in the proportional regime. Minimum ℓ_2 -norm solutions are also studied for other models, such as the kernel ridgeless regression (Liang & Rakhlin, 2020), classification (Chatterji & Long, 2021; Liang & Recht, 2021; Muthukumar et al., 2021), and the random feature model (Mei & Montanari, 2022).

2 Preliminaries

This section defines two types of random sketching matrices, introduces two out-of-sample prediction risks to measure the generalization performance, and presents various standing assumptions.

2.1 Sketching matrix

A sketching matrix $S \in \mathbb{R}^{m \times n}$ is used to obtain the sketched dataset $(S X, S Y)$ so that approximate computations can be done on the sketched dataset for the interest of the full dataset. We shall refer to $m < n$ as the sketching size and m/n the downsampling ratio. We consider two types of sketching matrices: the orthogonal and i.i.d. sketching matrices, defined below.

Definition 2.1 (Orthogonal sketching matrix). A sketching matrix S is an orthogonal sketching matrix if S is uniformly distributed over the space of all $m \times n$ partial orthogonal matrices, i.e., S is a random matrix with $S S^T = I_m$.

Definition 2.2 (i.i.d. sketching matrix). A sketching matrix S is an i.i.d. sketching matrix if it is composed of i.i.d. entries, each with mean zero, variance $1/n$, and a finite fourth moment.

For i.i.d. sketching, we consider i.i.d. Gaussian sketching matrices in all of our experiments, although our results hold for general i.i.d. sketching matrices. For orthogonal sketching, we construct an orthogonal sketching matrix based on the subsampled randomized Hadamard transforms (Ailon & Chazelle, 2006). Specifically, we use $S = BHDP$, where the rows of $B \in \mathbb{R}^{m \times n}$ are sampled without replacement from the standard basis of \mathbb{R}^n , $H \in \mathbb{R}^{n \times n}$ is a Hadamard matrix ^{*}, $D \in \mathbb{R}^{n \times n}$ is a diagonal matrix of i.i.d. Rademacher random variables, and $P \in \mathbb{R}^{n \times n}$ is a uniformly distributed permutation matrix. The time complexity of computing $(S X, S Y)$ is of order $O(np \log m)$. Orthogonal sketching matrices can also be realized by, for example, subsampling and Haar distributed matrices (Mezzadri, 2006).

2.2 Out-of-sample prediction risk

Recall that $\widehat{\beta}^S$ is the sketched ridgeless regression estimator defined in (1.2). Consider a test point $x_{\text{new}} \sim P_x$, independent of the training data. Following Hastie et al. (2022), we consider the following out-of-sample prediction risk as a measure of the generalization performance, defined as

$$R_{(\beta, S, X)}(\widehat{\beta}^S; \beta) = \mathbb{E} \left[(x_{\text{new}}^T \widehat{\beta}^S - x_{\text{new}}^T \beta)^2 \middle| \beta, S, X \right] = \mathbb{E} \left[\left\| \widehat{\beta}^S - \beta \right\|_{\Sigma}^2 \middle| \beta, S, X \right],$$

where $\Sigma := \text{cov}(x_i)$ is the covariance matrix of x_i and $\|x\|_{\Sigma}^2 := x^T \Sigma x$. We emphasize that the conditional expectation is taken with respect to the randomness of $\{\varepsilon_i\}_{1 \leq i \leq n}$ and x_{new} where β, S , and X are fixed. We have the following bias-variance decomposition

$$R_{(\beta, S, X)}(\widehat{\beta}^S; \beta) = B_{(\beta, S, X)}(\widehat{\beta}^S; \beta) + V_{(\beta, S, X)}(\widehat{\beta}^S; \beta), \quad (2.1)$$

where

$$B_{(\beta, S, X)}(\widehat{\beta}^S; \beta) = \left\| \mathbb{E}(\widehat{\beta}^S | \beta, S, X) - \beta \right\|_{\Sigma}^2, \quad (2.2)$$

$$V_{(\beta, S, X)}(\widehat{\beta}^S; \beta) = \text{tr} \left[\text{Cov}(\widehat{\beta}^S | \beta, S, X) \Sigma \right]. \quad (2.3)$$

We also consider a second out-of-sample prediction risk, defined as

$$R_{(S, X)}(\widehat{\beta}^S; \beta) = \mathbb{E} \left[(x_{\text{new}}^T \widehat{\beta}^S - x_{\text{new}}^T \beta)^2 \middle| S, X \right] = \mathbb{E} \left[\left\| \widehat{\beta}^S - \beta \right\|_{\Sigma}^2 \middle| S, X \right].$$

Compared with the first out-of-sample prediction risk, the second one also averages over the randomness of β . Similarly, we have the following bias-variance decomposition

$$R_{(S, X)}(\widehat{\beta}^S; \beta) = B_{(S, X)}(\widehat{\beta}^S; \beta) + V_{(S, X)}(\widehat{\beta}^S; \beta).$$

^{*}The definition of Hadamard matrices can be found, for example, in (Ailon & Chazelle, 2006).

where

$$B_{(S,X)}(\widehat{\beta}^S; \beta) = \mathbb{E} \left[\left\| \mathbb{E}(\widehat{\beta}^S | \beta, S, X) - \beta \right\|_{\Sigma}^2 | S, X \right], \quad (2.4)$$

$$V_{(S,X)}(\widehat{\beta}^S; \beta) = \mathbb{E} \left\{ \text{tr} \left[\text{Cov}(\widehat{\beta} | \beta, S, X) \Sigma \right] | S, X \right\}. \quad (2.5)$$

We shall also refer to the above out-of-sample prediction risks as test risks or simply risks, since they are the only risks considered in this paper. Throughout the paper, we study the above two out-of-sample prediction risks by studying the bias and variance terms respectively. Specifically, we study the behaviors of $R_{(\beta,S,X)}(\widehat{\beta}^S; \beta)$ and $R_{(S,X)}(\widehat{\beta}^S; \beta)$ in the proportional asymptotic limit where the sketching size m , sample size n , and dimensionality p all tend to infinity such that the original aspect ratio converges as $\phi_n := p/n \rightarrow \phi$ and the downsampling ratio converges as $\psi_n := m/n \rightarrow \psi \in (0, 1)$. Comparing with $R_{(S,X)}(\widehat{\beta}^S; \beta)$, the extra randomness in $R_{(\beta,S,X)}(\widehat{\beta}^S; \beta)$ introduced by the random β makes it exhibit larger variability.

2.3 Assumptions

This subsection collects standing assumptions.

Assumption 2.3 (Covariance and moment conditions). For $i = 1, \dots, n$, $x_i = \Sigma z_i$ where z_i has i.i.d. entries with mean zero, variance one and a finite moment of order $4 + \eta$ for some $\eta > 0$. The noise ε is independent of x , and follows a distribution P_{ε} on \mathbb{R} such that $\mathbb{E}(\varepsilon) = 0$ and $\text{Var}(\varepsilon) = \sigma^2$.

Assumption 2.4 (Random β). The coefficient vector β follows a multivariate normal distribution $\mathcal{N}_p(0, \frac{\sigma^2}{p} I_p)$, and is independent of the data matrix X , the noise ε , and the sketching matrix S .

Assumption 2.5 (Correlated features). Σ is a deterministic positive definite matrix, and there exists constants C_0, C_1 satisfying $0 < C_0 \leq \lambda_{\min}(\Sigma) \leq \lambda_{\max}(\Sigma) \leq C_1$ for all n, p . Define the empirical spectral distribution (ESD) of Σ as $F^{\Sigma}(x) = \frac{1}{p} \sum_{i=1}^p \mathbb{1}\{\lambda_i(\Sigma) \leq x\}$. Assume that as $p \rightarrow \infty$, the ESD F^{Σ} converges weakly to a probability measure H .

Assumption 2.6 (Sketching matrix). Let $S \in \mathbb{R}^{m \times n}$ be a sketching matrix. Suppose the ESD of SS^T converges weakly to a probability measure B . Furthermore, there exist constants $\widetilde{C}_0, \widetilde{C}_1 > 0$ such that almost surely for all large n , it holds that $0 < \widetilde{C}_0 \leq \lambda_{\min}(SS^T) \leq \lambda_{\max}(SS^T) \leq \widetilde{C}_1$.

Assumption 2.3 specifies the covariance structure for features and moment conditions for both features and errors (Dobriban & Wager, 2018; Hastie et al., 2022; Li et al., 2021). Dobriban & Liu (2018) only needs a finite fourth order moment of z_i , which is slightly weaker than the moment condition of ours. This is because they study the expected risk which has less randomness than our risks. In this paper, we first focus on the random β case as in Assumption 2.4, which assumes isotropic Gaussian distributions for β so that the

results on optimal sketching size can be presented in a clean manner. The random β assumption is commonly adopted in the literature (Dobriban & Wager, 2018; Li et al., 2021). We also consider the deterministic β in Section 6, where the interaction between β and Σ has to be taken into account. Assumption 2.6 on the sketching matrix is rather mild. For example, orthogonal sketching matrices satisfy this assumption naturally. According to Bai & Silverstein (1998), almost surely there is no eigenvalues outside the support of the limiting spectral distribution (LSD) of SS^\top for all sufficiently large n , thus the i.i.d. sketching matrices in Definition 2.2 also satisfy this assumption.

3 A warm-up case: Isotropic features

As a warm-up, we first study the case of isotropic features, i.e., $\Sigma = I_p$, and defer the general case to Section 4. Before presenting the limiting behaviors, we first relate the two out-of-sample prediction risks by presenting the following lemma, which is presented in terms of a general covariance matrix Σ .

Lemma 3.1. Under Assumptions 2.3 and 2.4, the two types of biases (2.2), (2.4) and variances (2.3), (2.5) have expressions

$$\begin{aligned} B_{(\beta, S, X)}(\widehat{\beta}^S; \beta) &= \beta^\top \left[(X^\top S^\top S X)^+ X^\top S^\top S X - I_p \right] \Sigma \left[(X^\top S^\top S X)^+ X^\top S^\top S X - I_p \right] \beta, \\ B_{(S, X)}(\widehat{\beta}^S; \beta) &= \frac{\alpha^2}{p} \text{tr} \left\{ \left[I_p - (X^\top S^\top S X)^+ X^\top S^\top S X \right] \Sigma \right\}, \\ V_{(\beta, S, X)}(\widehat{\beta}^S; \beta) &= V_{(S, X)}(\widehat{\beta}^S; \beta) = \text{tr} \left[\sigma^2 (X^\top S^\top S X)^+ X^\top S^\top S S^\top S X (X^\top S^\top S X)^+ \Sigma \right]. \end{aligned}$$

Furthermore, suppose there exists C_1 such that $\lambda_{\max}(\Sigma) \leq C_1$. Then as $n, p \rightarrow \infty$,

$$R_{(\beta, S, X)}(\widehat{\beta}^S; \beta) - R_{(S, X)}(\widehat{\beta}^S; \beta) \xrightarrow{\text{a.s.}} 0. \quad (3.1)$$

The above lemma indicates that the two risks are asymptotically equivalent when β is random. Specifically, the variance terms are exactly equal to each other while the bias terms agree asymptotically. Because of this asymptotic equivalence, we only need to focus on $R_{(S, X)}(\widehat{\beta}^S; \beta)$ when studying the asymptotic risks. We point out that the second order inferential results do not agree in general, which will be discussed in detail in Section 6.

3.1 Limiting risks

We first focus on the case of $\Sigma = I_p$, in which the limiting risks have clean formulae. We characterize the limiting risks with two types of sketching matrices: the orthogonal and i.i.d. sketching matrices, as introduced before. Recall $m, n, p \rightarrow \infty$ such that $p/n \rightarrow \phi$ and $m/n \rightarrow \psi \in (0, 1)$.

Theorem 3.2. Assume Assumptions 2.3, 2.4, and 2.6 and $\Sigma = I_p$. The followings hold.

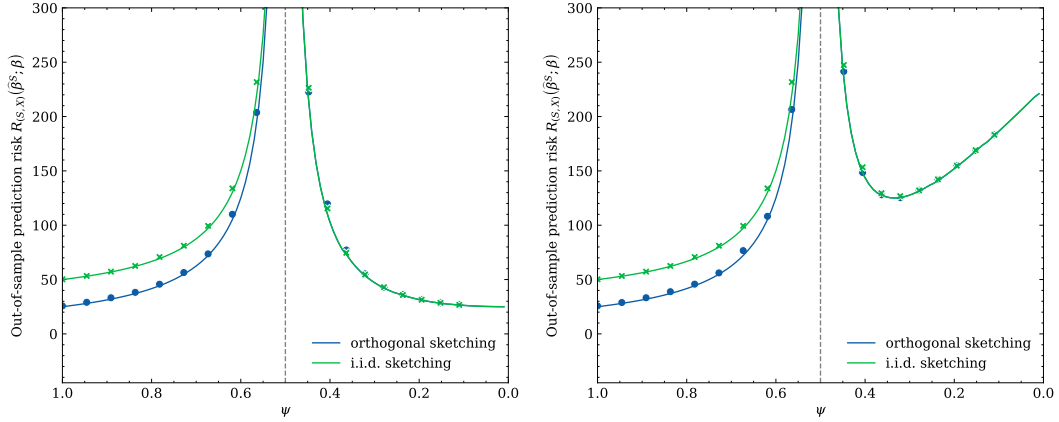


Figure 2: Asymptotic risk curves for sketched ridgeless least square estimators with isotropic features, orthogonal or i.i.d. sketching, as functions of ψ . The lines in the left panel are theoretical risk curves for orthogonal and i.i.d. sketching, $\text{SNR} = \alpha/\sigma = 1$ with $(\alpha, \sigma) = (5, 5)$, while the lines in the right panel are theoretical risk curves for $\text{SNR} = \alpha/\sigma = 3$ with $(\alpha, \sigma) = (15, 5)$. The dots and crosses mark finite-sample risks for orthogonal sketching and i.i.d. sketching respectively, with $n = 400$, $p = 200$, ψ varying in $(0, 1)$, and $m = [n\psi]$. Each row of $X \in \mathbb{R}^{n \times p}$ was i.i.d. drawn from $\mathcal{N}_p(0, I_p)$. Orthogonal sketching matrices S were drawn uniformly such that $SS^\top = I_m$; each entry of i.i.d. sketching matrices S were drawn from normal distribution with mean 0 and variance $1/n$.

(i) If S is an orthogonal sketching matrix, then

$$R_{(S,X)}(\hat{\beta}^S; \beta) \xrightarrow{\text{a.s.}} \begin{cases} \frac{\sigma^2 \phi \psi^{-1}}{1 - \phi \psi^{-1}}, & \phi \psi^{-1} < 1, \\ \alpha^2 (1 - \psi \phi^{-1}) + \frac{\sigma^2}{\phi \psi^{-1} - 1}, & \phi \psi^{-1} > 1. \end{cases}$$

(ii) If S is an i.i.d. sketching matrix, then

$$R_{(S,X)}(\hat{\beta}^S; \beta) \xrightarrow{\text{a.s.}} \begin{cases} \frac{\sigma^2 \phi}{1 - \phi} + \frac{\sigma^2 \phi \psi^{-1}}{1 - \phi \psi^{-1}}, & \phi \psi^{-1} < 1, \\ \alpha^2 (1 - \psi \phi^{-1}) + \frac{\sigma^2}{\phi \psi^{-1} - 1}, & \phi \psi^{-1} > 1. \end{cases}$$

Moreover, $R_{(\beta,S,X)}(\hat{\beta}^S; \beta)$ converges almost surely to the same limits respectively.

The above theorem characterizes the limiting risks of sketched ridgeless least square estimators with both orthogonal and i.i.d. sketching. The limiting risks are characterized by theoretical risk curves in both the underparameterized regime after sketching, aka $\phi \psi^{-1} < 1$, and the overparameterized regime after sketching, aka $\phi \psi^{-1} > 1$. We shall refer to the underparameterized and overparameterized regimes after sketching as underparameterized and overparameterized regimes for simplicity.

Perhaps surprisingly, orthogonal and i.i.d. sketching exhibit different phenomena in the underparameterized regime but agree in the overparameterized regime. In the underparameterized regime, taking orthogonal sketching is strictly better than taking i.i.d. sketching in

terms of limiting risks. This is perhaps because i.i.d. sketching distorts the geometry of least square regression estimator due to the non-orthogonality, which was first pointed out by [Dobriban & Liu \(2018\)](#) but for a different risk. Specifically, their risk is the expected version of ours and thus Theorem 3.2 can recover their results in the underparameterized case by using the dominated convergence theorem. Moving to the overparameterized case, however, taking orthogonal and i.i.d. sketching leads to identical limiting risks. Specifically, when $\phi\psi^{-1} > 1$, the bias term $B_{(S,X)}(\widehat{\beta}^S; \beta) \xrightarrow{\text{a.s.}} \alpha^2(1 - \psi\phi^{-1})$ and the variance term $V_{(S,X)}(\widehat{\beta}^S; \beta) \xrightarrow{\text{a.s.}} \sigma^2(\phi\psi^{-1} - 1)^{-1}$ hold for both types of sketching.

Let $\text{SNR} = \alpha/\sigma$. Figure 2 plots asymptotic risk curves for sketched ridgeless least square estimators with orthogonal or i.i.d. sketching when $\text{SNR} = \alpha/\sigma = 1, 3$ with $(\alpha, \sigma) = (5, 5)$, and $(\alpha, \sigma) = (15, 5)$ respectively, as functions of ψ , as well as finite-sample risks. As shown in the figure, taking orthogonal sketching is strictly better than taking i.i.d. sketching in the underparameterized regime while they are identical to each other in the overparameterized regime.

To close this subsection, we compare the limiting risk $R_{(S,X)}(\widehat{\beta}; \beta)$ of the orthogonally sketched estimator with that of the full-sample one, since orthogonal sketching is universally better than i.i.d. sketching. A variant of ([Hastie et al., 2022](#), Theorem 1) gives the limiting risk $R_{(S,X)}(\widehat{\beta}; \beta)$ of the full-sample ridgeless least square estimator $\widehat{\beta}$ with isotropic features:

$$R_{(S,X)}(\widehat{\beta}; \beta) \xrightarrow{\text{a.s.}} \begin{cases} \frac{\sigma^2\phi}{1 - \phi}, & \phi < 1, \\ \alpha^2(1 - \phi) + \frac{\sigma^2}{\phi - 1}, & \phi > 1. \end{cases}$$

Figure 1 plots asymptotic risk curves and finite-sample risks. The limiting risk $R_{(S,X)}(\widehat{\beta}; \beta)$ depends on the sample size n and dimensionality p only through the aspect ratio $\phi = p/n$. Comparing the limiting risk above with that of the orthogonally sketched estimator in Theorem 3.2, orthogonal sketching affects the limiting risk by changing the *effective aspect ratio* from $\phi = \lim p/n$ for the original problem to $\phi\psi^{-1} = \lim p/m$ for the sketched problem. This is somewhat natural as sketching is a form of downsampling which affects the aspect ratio and thus the limiting risk. It is natural to ask the following question:

By carefully choosing the sketching size, can we possibly improve the out-of-sample prediction risks and thus the generalization performance?

This seems possible as the asymptotic risk curves in Figure 1 are not monotone. In what follows, we study what the optimal sketching size is.

3.2 Optimal sketching size

Following the discussion in the last subsection, we discuss how to pick the optimal sketching size m^* to minimize the limiting risks for both orthogonal and i.i.d. sketching.

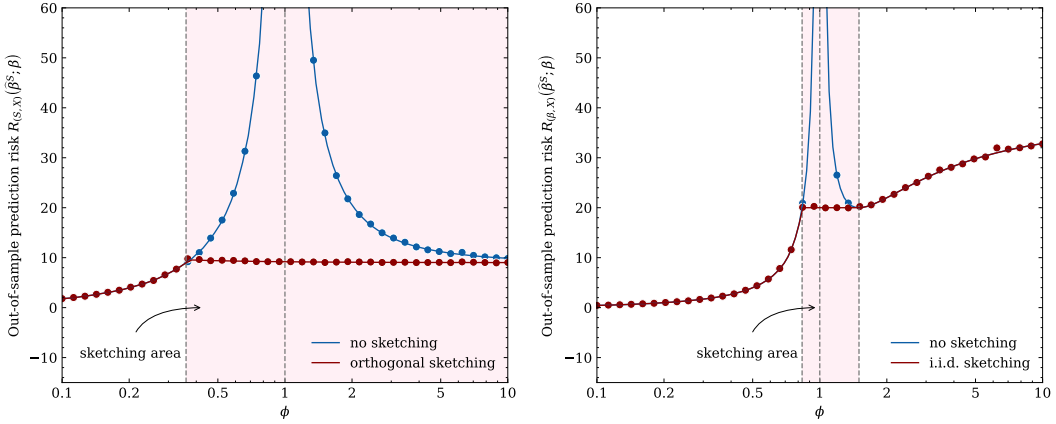


Figure 3: Asymptotic risk curves for the full-sample (no sketching) and sketched ridgeless least square estimators with isotropic features and orthogonal or i.i.d. sketching, as functions of ϕ . For the sketched estimator, an optimal sketching size m^* is selected based on SNR and ϕ , as described in Theorem 3.3. The red line and blue line are theoretical risk curves for sketched estimator and non-sketched estimator, respectively. The dots mark finite-sample risks with $n = 400$, ϕ varying in $[0.1, 10]$, and $p = [n\phi]$. The left panel shows the case for $\text{SNR} = \alpha/\sigma = 0.75$ with $(\alpha, \sigma) = (3, 4)$, while the right panel shows the case for $\text{SNR} = \alpha/\sigma = 3$ with $(\alpha, \sigma) = (6, 2)$. The feature, orthogonal sketching, and i.i.d. sketching matrices were generated the same way as in Figure 2.

Theorem 3.3 (Optimal sketching size for orthogonal and i.i.d. sketching). Assume Assumptions 2.3, 2.4, and 2.6 and $\Sigma = I_p$. We can determine the optimal size m^* in all cases regarding the SNR and the aspect ratio ϕ as follows.

- (a) If $\text{SNR} > 1$ and $\phi \in (1 - \frac{\sigma}{2\alpha}, \frac{\alpha}{\alpha-\sigma}]$, the optimal sketching size to minimize both limiting risks is $m^* = \frac{\alpha-\sigma}{\alpha}\phi \cdot n$.
- (b) If $\text{SNR} \leq 1$ and $\phi \in (\frac{\alpha^2}{\alpha^2+\sigma^2}, \infty)$, the optimal sketching size to minimize both limiting risks is $m^* \ll n$.
- (c) No sketching is needed if either of the following two holds: (i) $\text{SNR} \leq 1$ and $\phi \in (0, \frac{\alpha^2}{\alpha^2+\sigma^2}]$, or (ii) $\text{SNR} > 1$ and $\phi \in (0, 1 - \frac{\sigma}{2\alpha}] \cup (\frac{\alpha}{\alpha-\sigma}, \infty)$.

Theorem 3.3 indicates that both orthogonal and i.i.d. sketching can help improve the out-of-sample prediction risks in some cases. Specifically, when the signal-to-noise ratio is large with $\text{SNR} > 1$ and the aspect ratio is neither too large nor too small with $\phi \in (1 - \sigma/(2\alpha), \alpha/(\alpha - \sigma)]$, a nontrivial sketching size $m^* = (\alpha - \sigma)\phi n/\alpha$ leads to the optimal asymptotic risk. When the signal-to-noise ratio is low and the problem dimension is large, the null estimator $\tilde{\beta} = 0$ is the best among all sketched ridgeless least square estimators, which corresponds to $m^* \ll n$.

Figure 3 plots asymptotic risk curves for the full-sample and the optimally sketched ridgeless least square estimators with isotropic features, orthogonal or i.i.d. sketching, as functions of ϕ . As can be seen from the figure, optimal sketching can stabilize the asymptotic risk curve by eliminating the peaks, which implies the optimally sketched estimator

is a more stable estimator than the full-sample one. In Section 5, we propose a practical procedure to pick the optimally sketched estimator.

4 Correlated features

Instead of assuming $\Sigma = I_p$, this section considers a general positive definite Σ . Most of our results apply to general sketching matrices, including orthogonal and i.i.d. sketching as special cases. In what follows, we present results in the overparameterized and underparameterized cases respectively.

4.1 Overparameterized regime

Recall that H is the limiting spectral distribution (LSD) of Σ , and $p, m, n \rightarrow \infty$ such that $\phi_n = p/n \rightarrow \phi$ and $\psi_n = m/n \rightarrow \psi \in (0, 1)$. To study the overparameterized case, we need the following lemma.

Lemma 4.1. Assume Assumption 2.5. Suppose $\phi\psi^{-1} > 1$. Then the following equation (4.1) has a unique negative solution with respect to c_0 ,

$$1 = \int \frac{x}{-c_0 + x\psi\phi^{-1}} dH(x). \quad (4.1)$$

The result above establishes that there exists a unique negative solution to the equation (4.1). Equations of the type (4.1) are often referred to as self-consistent equations (Bai & Silverstein, 2010), which do not necessarily admit closed-form solutions but can be computed numerically. These equations play important roles in calculating the asymptotic asymptotic risks. Lemma 4.1 shows the existence and uniqueness of the solution to (4.1) over \mathbb{R}^- , where \mathbb{R}^- is the negative real line. This result is required for our asymptotic risk calculations but is not available in the literature to the best of our knowledge. From now on, denote $c_0 = c_0(\phi, \psi, H)$ as the unique negative solution to (4.1). Our next result characterizes the limiting risks as well as the limiting biases and variances in the overparameterized regime.

Theorem 4.2. Assume Assumptions 2.3, 2.4, 2.5 and 2.6. Suppose $\phi\psi^{-1} > 1$. Then

$$B_{(S,X)}(\widehat{\beta}^S; \beta), B_{(\beta,S,X)}(\widehat{\beta}^S; \beta) \xrightarrow{\text{a.s.}} -\alpha^2 c_0, \quad (4.2)$$

$$V_{(S,X)}(\widehat{\beta}^S; \beta) = V_{(\beta,S,X)}(\widehat{\beta}^S; \beta) \xrightarrow{\text{a.s.}} \sigma^2 \frac{\int \frac{x^2\psi\phi^{-1}}{(c_0-x\psi\phi^{-1})^2} dH(x)}{1 - \int \frac{x^2\psi\phi^{-1}}{(c_0-x\psi\phi^{-1})^2} dH(x)}. \quad (4.3)$$

Consequently, both $R_{(S,X)}(\widehat{\beta}^S; \beta)$ and $R_{(\beta,S,X)}(\widehat{\beta}^S; \beta)$ converge almost surely to the sum of right hand sides of (4.2) and (4.3).

Different from the case with isotropic features, the asymptotic risk does not admit close form solutions. They can be, however, computed numerically. When $\Sigma = I_p$, H degenerates

to the Dirac measure $\delta_{\{1\}}$. Some simple algebra shows $c_0 = \psi\phi^{-1} - 1$, and $B_{(S,X)}(\widehat{\beta}^S; \beta) \rightarrow \alpha^2(1 - \psi\phi^{-1})$, $V_{(S,X)}(\widehat{\beta}^S; \beta) \rightarrow \frac{\sigma^2}{\phi\psi^{-1}-1}$, which coincides with the results in Theorem 3.2. Moreover, in the overparameterized regime, the limiting risks do not depend on a specific sketching matrix, which generalizes the same phenomenon indicated by Theorem 3.2 for isotropic features.

4.2 Underparameterized regime

Recall that H is the limiting spectral distribution of SS^T . Let $\tilde{c}_0 = \tilde{c}_0(\phi, \psi, B)$ be the unique negative solution of the following self-consistent equation

$$1 = \psi \int \frac{x}{-\tilde{c}_0 + x\phi} dB(x). \quad (4.4)$$

The following result presents the limiting risks in the underparameterized regime as well as their limiting biases and variances.

Theorem 4.3. Suppose Assumptions 2.3, 2.4, 2.5 and 2.6. Suppose $\phi\psi^{-1} < 1$. Then

$$B_{(S,X)}(\widehat{\beta}^S; \beta), B_{(\beta,S,X)}(\widehat{\beta}^S; \beta) \xrightarrow{\text{a.s.}} 0, \quad (4.5)$$

$$V_{(S,X)}(\widehat{\beta}^S; \beta) = V_{(\beta,S,X)}(\widehat{\beta}^S; \beta) \xrightarrow{\text{a.s.}} \sigma^2 \frac{\psi \int \frac{x^2\phi}{(\tilde{c}_0-x\phi)^2} dB(x)}{1 - \psi \int \frac{x^2\phi}{(\tilde{c}_0-x\phi)^2} dB(x)}. \quad (4.6)$$

Consequently, both $R_{(S,X)}(\widehat{\beta}^S; \beta)$ and $R_{(\beta,S,X)}(\widehat{\beta}^S; \beta)$ converge almost surely to the right hand side of (4.6).

In the underparameterized case, the bias terms vanish and the variance terms depend on the sketching matrix S and is independent of the covariance matrix Σ . The following corollary presents the limiting variances of orthogonal and i.i.d. sketching.

Corollary 4.4. Assume the same assumptions in Theorem 4.3. The followings hold.

(i) If S is a orthogonal sketching matrix, then

$$V_{(S,X)}(\widehat{\beta}^S; \beta) = V_{(\beta,S,X)}(\widehat{\beta}^S; \beta) \xrightarrow{\text{a.s.}} \sigma^2 \frac{\phi\psi^{-1}}{1 - \phi\psi^{-1}}. \quad (4.7)$$

(ii) If S is an i.i.d. sketching matrix, then

$$V_{(S,X)}(\widehat{\beta}^S; \beta) = V_{(\beta,S,X)}(\widehat{\beta}^S; \beta) \xrightarrow{\text{a.s.}} \sigma^2 \left(\frac{\phi}{1 - \phi} + \frac{\phi\psi^{-1}}{1 - \phi\psi^{-1}} \right). \quad (4.8)$$

The corollary above indicates again that taking i.i.d. sketching yields a larger limiting variance than taking orthogonal sketching, which generalizes the corresponding results for isotropic features. One may naturally wonder:

Is orthogonal sketching matrix optimal among all sketching matrices?

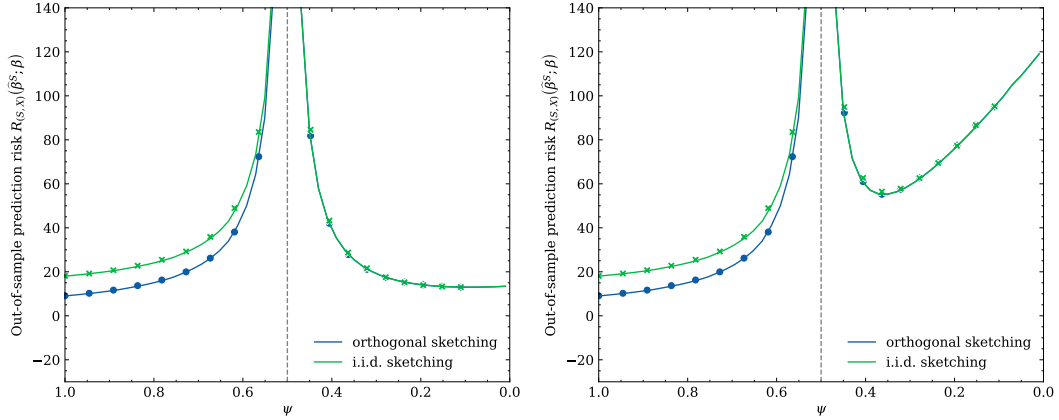


Figure 4: Asymptotic risk curves for sketched ridgeless least square estimators with correlated features, orthogonal or i.i.d. sketching, as functions of ψ . The lines in the left panel are theoretical risk curves for orthogonal and i.i.d. sketching, $\text{SNR} = \alpha/\sigma = 1$ with $(\alpha, \sigma) = (3, 3)$, while the lines in the right panel are theoretical risk curves for $\text{SNR} = \alpha/\sigma = 3$ with $(\alpha, \sigma) = (9, 3)$. The dots and crosses mark finite-sample risks for orthogonal sketching and i.i.d. sketching respectively with $n = 400$, $p = 200$, ψ varying in $(0, 1)$, and $m = [n\psi]$. Each row of $X \in \mathbb{R}^{n \times p}$ was i.i.d. drawn from $\mathcal{N}_p(0, \Sigma)$ and Σ has empirical spectral distribution $F^\Sigma(x) = \frac{1}{p} \sum_{i=1}^p \mathbb{1}\{\lambda_i(\Sigma) \leq x\}$ with $\lambda_i = 2$ for $i = 1, \dots, [p/2]$, and $\lambda_i = 1$ for $i = [p/2] + 1, \dots, p$. The orthogonal and i.i.d. sketching matrices were generated the same way as in Figure 2.

We give a positive answer to the above question by leveraging the variance formula (4.6). Specifically, the following result shows that the dirac measure, which corresponds to orthogonal sketching, minimizes the variance formula (4.6) and thus the limiting risks.

Corollary 4.5 (Optimal sketching matrix). Consider ϕ and ψ fixed. Taking $B = \delta_{\{a\}}$ with some $a > 0$, which corresponds to orthogonal sketching, can minimize the limiting variance (4.6), and thus the limiting risks, over all B 's that are supported on the positive real line $\mathbb{R}_{>0}$.

Figure 4 plots the asymptotic risk curves for sketched ridgeless least square estimators with correlated features, orthogonal or i.i.d. sketching, as functions of ψ . It shows that, for a slightly more general Σ , taking orthogonal sketching is strictly better than taking i.i.d. sketching in the underparameterized regime while they are identical in the overparameterized regime. Figure 5 compares the full-sample and sketched least square estimators, which indicates that both orthogonal and i.i.d. sketching can make the risk curve stabler by eliminating the peaks in the risk curves.

5 A practical procedure

Picking the optimal sketching size based on the theoretical risk curves requires the knowledge of SNR, which is often unknown in practice. Thus selecting the optimal sketching size m^* requires new and probably complicated methodologies for estimating the SNR, which is beyond the scope of this work. In this section, we provide a simple yet practical procedure

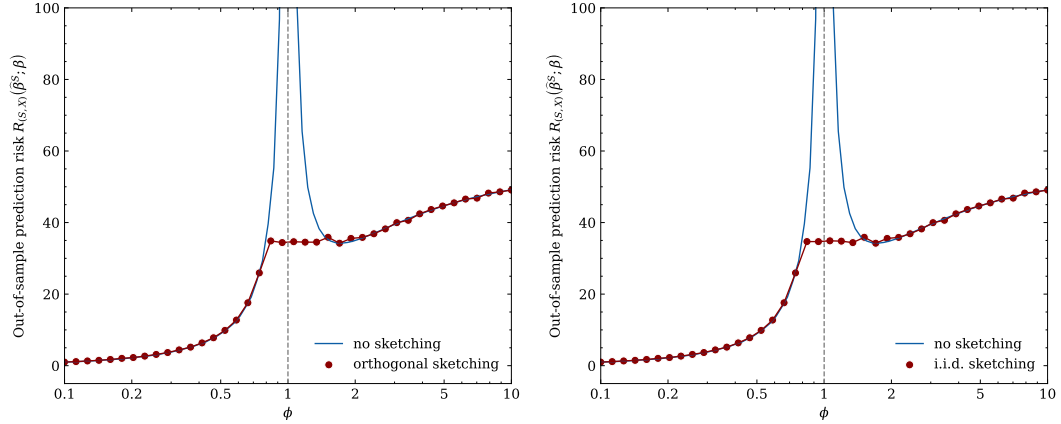


Figure 5: Asymptotic risk curves for the full-sample (no sketching) and sketched ridgeless least square estimators with correlated features, orthogonal sketching or i.i.d. sketching, as functions of ϕ . For the sketched estimator, an optimal sketching size m^* is selected based on theoretical risk curves (see Appendix A.2 for more details). The blue lines are theoretical risk curves for non-sketched estimators with $\text{SNR} = \alpha/\sigma = 2$ where $(\alpha, \sigma) = (6, 3)$. The red dots mark finite-sample risks of sketched estimators with $n = 400$, ϕ varying in $[0.1, 10]$, and $p = [n\phi]$. The feature, orthogonal sketching, and i.i.d. sketching matrices were generated the same way as in Figure 4.

to pick the best possible sketching size, provided we have access to an additional validation dataset. This is not very restrictive especially in applications with big and streaming data where a validation dataset can be easily obtained. Otherwise, we can manually split the dataset into two parts: a training dataset and a validation dataset. The training dataset is used to obtain the sketched estimators while the validation dataset is used to pick the best sketching size. The test risk $R_{(S,X)}(\hat{\beta}^S; \beta)$ can then be evaluated on the testing dataset using the tuned sketched least square estimator.

Numerical studies were used to evaluate the performance of the above procedure. We run 500 replications. For each replication, we generated $\beta \sim \mathcal{N}_p(0, \frac{\alpha^2}{p} I_p)$ and a training dataset (X, Y) with $n = 400$ training samples, a validation dataset $\{(x_{\text{val},i}, y_{\text{val},i}) : 1 \leq i \leq n_{\text{val}}\}$ with $n_{\text{val}} = \{20, 100, 200\}$ validation samples, and a testing dataset $\{(x_{\text{new},i}, y_{\text{new},i}) : 1 \leq i \leq n_{\text{new}}\}$ with $n_{\text{new}} = 100$ testing samples. The feature matrix $X \in \mathbb{R}^{n \times p}$, orthogonal sketching, and i.i.d. sketching matrices were generated the same way as in Figure 5, and were fixed across all replications. Next, we provide details on how sketching size was selected in each replication and how empirical out-of-sample prediction risks were calculated.

Selection of the optimal sketching size. The empirically optimal sketching size \hat{m} was selected if it minimized the empirical risks across a set of values for m evaluated on the validation dataset. Specifically, given fixed p and n , we varied ψ by taking a grid of $\psi \in (0, 1)$ with $|\psi_i - \psi_{i+1}| = \delta$ for $\delta = 0.05$. This led to a set of potential values for \hat{m} , i.e., $m_i = [\psi_i n]$. For each m_i , we fitted a sketched ridgeless least square estimator $\hat{\beta}^{S_{m_i}}$ using the

training dataset and calculated the empirical risks on the validation dataset:

$$\widehat{R}_{(S_{m_i}, X)}^{\text{val}}(\widehat{\beta}^{S_{m_i}}; \beta) = \frac{1}{n_{\text{val}}} \sum_{i=1}^{n_{\text{val}}} (x_{\text{val}, i}^T \widehat{\beta}^{S_{m_i}} - x_{\text{val}, i}^T \beta)^2. \quad (5.1)$$

The empirical optimal sketching size \widehat{m} was picked as the one that minimized the empirical risks across all m_i .

Evaluation of the out-of-sample prediction performance. In the k -th replication, we first generate the coefficient vector $\beta(k)$ if the empirically best sketching size was $\widehat{m}(k) = n$, we fitted a ridgeless least square estimator $\widehat{\beta}(k)$ on the training set; if $\widehat{m}(k) < n$, we fitted a sketched ridgeless least square estimator with the selected $\widehat{m}(k)$. Denote this final estimator by $\widehat{\beta}(k)^{S_{\widehat{m}(k)}}$. The empirical risk of this final estimator was then evaluated on the testing dataset:

$$\widehat{R}_{(S, X)}(\widehat{\beta}^S; \beta) = \frac{1}{500} \sum_{k=1}^{500} \left\{ \frac{1}{n_{\text{new}}} \sum_{r=1}^{n_{\text{new}}} (x_{\text{new}, r}^T \widehat{\beta}(k)^{S_{\widehat{m}(k)}} - x_{\text{new}, r}^T \beta(k))^2 \right\}. \quad (5.2)$$

Figure 6 plots the asymptotic risk curves for the full-sample and sketched least square estimators with orthogonal sketching, correlated features, and the the theoretically and empirically optimal sketching sizes. The performance of the orthogonal sketched estimator with \widehat{m} is comparable to that of sketched estimators with m^* when $n_{\text{val}} = \{20, 100, 200\}$. As the size of the validation dataset increases, the finite-sample risk curve of the orthogonally sketched estimator with \widehat{m} becomes stabler and closer to that of the orthogonally sketched estimator with m^* . Moreover, a particularly small validation dataset with $n_{\text{val}} = 20$ already suffices for producing an estimator with a stable and monotone risk curve.

6 Extensions

6.1 Deterministic β case

Previously, we assume that the coefficient vector β is independent of the data matrix X and follows a multivariate normal distribution $\mathcal{N}_p(0, \frac{\alpha^2}{p} I_p)$. This section considers deterministic β as specified in the following assumption.

Assumption 6.1 (Deterministic β). The coefficient vector β is deterministic.

Denote the eigenvalue decomposition of Σ by $\Sigma = \sum_{i=1}^p \lambda_i u_i u_i^T$ where, under Assumption 2.5, $C_1 \geq \lambda_1 \geq \lambda_2 \geq \dots \geq \lambda_p \geq C_0 > 0$. We define the eigenvector empirical spectral distribution (VESD) to be

$$G_n(x) = \frac{1}{\|\beta\|^2} \sum_{i=1}^p \langle \beta, u_i \rangle^2 \mathbb{1}\{\lambda_i \leq x\}, \quad (6.1)$$

which characterizes the relation of Σ and β . Theorem 6.2 presents the asymptotic risk when β is deterministic. According to the Lemma 3.1, the variance term is exactly the same as in

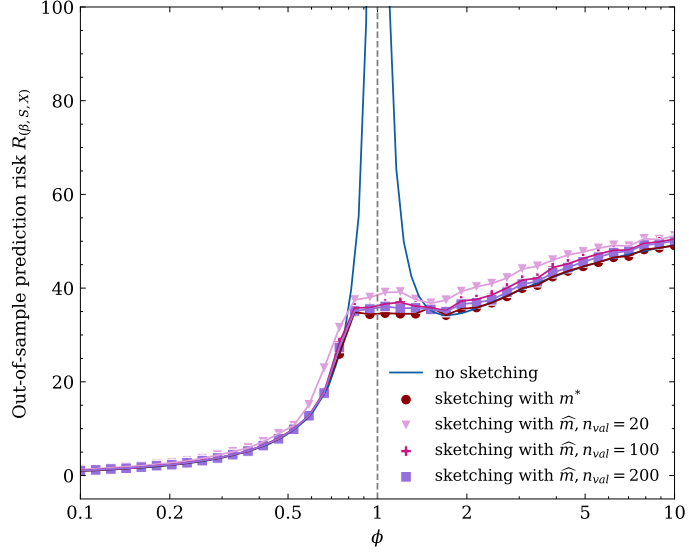


Figure 6: Asymptotic risk curves for the full-sample (no sketching) and sketched ridgeless least square estimators with correlated features and orthogonal sketching as functions of ϕ . The blue line is theoretical risk curves for non-sketched estimators with $\text{SNR} = \alpha/\sigma = 2$ where $(\alpha, \sigma) = (6, 3)$. The red dots mark finite-sample risks of sketched estimators with the theoretically optimal sketching size m^* , while the plum triangles, pink crosses, and purple squares mark finite-sample risks of sketched estimators with the empirically optimal sketching size \hat{m} picked by the validation sets with $n_{\text{val}} = 20, n_{\text{val}} = 100, n_{\text{val}} = 200$, where $n = 400$, ϕ varies in $[0.1, 10]$, and $p = [n\phi]$. The feature and orthogonal sketching matrices were generated the same way as in Figure 5.

the previous two subsections. Besides, the bias vanishes in the under-parameterized regime. Thus, the only nontrivial case is the bias for the over-parameterized case. Let

$$c_1 := \frac{\int \frac{x^2 \psi \phi^{-1}}{(c_0 - x \psi \phi^{-1})^2} dH(x)}{1 - \int \frac{x^2 \psi \phi^{-1}}{(c_0 - x \psi \phi^{-1})^2} dH(x)} \quad (6.2)$$

where c_0 is defined in (4.1). The c_1 can be treated as a rescaled limiting variance of the sketched estimator in the overparameterized regime; see (4.3).

Theorem 6.2. Assume Assumptions 2.3, 2.5, 2.6, and 6.1. Then the followings hold.

(i) If $p/m \rightarrow \phi \psi^{-1} < 1$,

$$B_{(\beta,S,X)}(\widehat{\beta}^S; \beta) \xrightarrow{\text{a.s.}} 0. \quad (6.3)$$

(ii) If $p/m \rightarrow \phi \psi^{-1} > 1$ and assume the VESD G_n defined in (6.1) converges weakly to a probability measure G , then

$$B_{(\beta,S,X)}(\widehat{\beta}^S; \beta) / \|\beta\|^2 \xrightarrow{\text{a.s.}} (1 + c_1) \int \frac{c_0^2 x}{(c_0 - x \psi \phi^{-1})^2} dG(x). \quad (6.4)$$

For the variance term, $V_{(\beta, S, X)}(\widehat{\beta}^S; \beta)$ converges to the same limit as (4.3) and (4.6) respectively for the over-parameterized and under-parameterized cases.

Hastie et al. (2022) obtained a similar result in the case of the full-sample ridgeless least square estimator. Because we are dealing with sketched estimators where additional random sketching matrices are involved, our proofs are more challenging. Specifically, we utilize results for separable covariance matrices. If we further assume $\|\beta\|^2 \rightarrow \alpha^2$ and $\Sigma = I_p$, then Theorem 6.2 shall recover the same limiting risks in Theorem 3.2.

6.2 Central limit theorem

This subsection establishes central limit theorems for both out-of-sample prediction risks $R_{(\beta, S, X)}(\widehat{\beta}^S; \beta)$ and $R_{(S, X)}(\widehat{\beta}^S; \beta)$. Li et al. (2021) studies the central limit theorems for risks of full-sample ridgeless least square estimator. Compared with their work, our results show the risks of sketched estimators may have smaller asymptotic variances. We start with the following assumption.

Assumption 6.3. Suppose $\{X_{ij}\}$ share the fourth moment $\nu_4 := \mathbb{E}|X_{ij}|^4 < \infty$. Furthermore, they satisfy the following Lindeberg condition

$$\frac{1}{np} \sum_{1 \leq i \leq n, 1 \leq j \leq p} \mathbb{E}(|X_{ij}|^4 \mathbf{1}_{\{|X_{ij}| \geq \eta \sqrt{n}\}}) \rightarrow 0, \quad \text{for any fixed } \eta > 0.$$

CLTs for $R_{(S, X)}(\widehat{\beta}^S; \beta)$. The following theorems give CLTs for $R_{(S, X)}(\widehat{\beta}^S; \beta)$ in the under-parameterized and overparameterized regimes. Recall that $m, n, p \rightarrow \infty$ such that $\phi_n = p/n \rightarrow \phi$ and $\psi_n = m/n \rightarrow \psi \in (0, 1)$.

Theorem 6.4. Assume Assumptions 2.3, 2.4, 2.5, 2.6 and 6.3. Suppose $\phi\psi^{-1} < 1$ and S is an orthogonal sketching matrix. Then it holds that

$$p \left(R_{(S, X)}(\widehat{\beta}^S; \beta) - \frac{\sigma^2 \phi_n \psi_n^{-1}}{1 - \phi_n \psi_n^{-1}} \right) \xrightarrow{D} \mathcal{N}(\mu_1, \sigma_1^2),$$

where

$$\mu_1 = \frac{\sigma^2 \phi^2 \psi^{-2}}{(\phi\psi^{-1} - 1)^2} + \frac{\sigma^2 \phi^2 \psi^{-2} (\nu_4 - 3)}{1 - \phi\psi^{-1}}, \quad \sigma_1^2 = \frac{2\sigma^4 \phi^3 \psi^{-3}}{(\phi\psi^{-1} - 1)^4} + \frac{\sigma^4 \phi^3 \psi^{-3} (\nu_4 - 3)}{(1 - \phi\psi^{-1})^2}.$$

Theorem 6.5. Assume Assumptions 2.3, 2.4, 6.3 and $\Sigma = I_p$. Suppose $\phi\psi^{-1} > 1$ and S is any sketching matrix that satisfies Assumption 2.6. Then it holds that

$$p \left(R_{(S, X)}(\widehat{\beta}^S; \beta) - \alpha^2 (1 - \psi_n \phi_n^{-1}) - \frac{\sigma^2}{\phi_n \psi_n^{-1} - 1} \right) \xrightarrow{D} \mathcal{N}(\mu_2, \sigma_2^2),$$

where

$$\mu_2 = \frac{\sigma^2 \phi \psi^{-1}}{(\phi\psi^{-1} - 1)^2} + \frac{\sigma^2 (\nu_4 - 3)}{\phi\psi^{-1} - 1}, \quad \sigma_2^2 = \frac{2\sigma^4 \phi^3 \psi^{-3}}{(\phi\psi^{-1} - 1)^4} + \frac{\sigma^4 \phi \psi^{-1} (\nu_4 - 3)}{(\phi\psi^{-1} - 1)^2}.$$

The CLT of $R_{(S,X)}(\widehat{\beta}^S; \beta)$ after an orthogonal sketching $(X, Y) \mapsto (SX, SY)$ coincides with that by [Li et al. \(2021\)](#) after replacing p/n by p/m . According to Theorems [6.4](#), [6.5](#) and [3.3](#), we provide the asymptotic variance of $R_{(S,X)}(\widehat{\beta}^S; \beta)$ for the orthogonal sketched estimator with the optimal sketching size m^* given by Theorem [3.3](#).

Corollary 6.6. Denote the asymptotic variance of the risk $R_{(S,X)}(\widehat{\beta}^S; \beta)$ for the orthogonal sketched estimator with the optimal sketching size m^* by σ_S^2 . The followings hold.

- (a) If $\text{SNR} > 1$ and $\phi \in (1 - \frac{\sigma}{2\alpha}, \frac{\alpha}{\alpha-\sigma}]$, then $\sigma_S^2 = 2\alpha^3(\alpha - \sigma) + \sigma^2(\nu_4 - 3)\alpha(\alpha - \sigma)$.
- (b) If $\text{SNR} \leq 1$ and $\phi \in (\frac{\alpha^2}{\alpha^2+\sigma^2}, \infty)$, then $\sigma_S^2 = O(\frac{m^*}{n}) \rightarrow 0$.
- (c) If either of the following two holds: (i) $\text{SNR} \leq 1$ and $\phi \in (0, \frac{\alpha^2}{\alpha^2+\sigma^2}]$, or (ii) $\text{SNR} > 1$ and $\phi \in (0, 1 - \frac{\sigma}{2\alpha}] \cup (\frac{\alpha}{\alpha-\sigma}, \infty)$, then

$$\sigma_S^2 = \begin{cases} \frac{2\sigma^4\phi^3}{(\phi-1)^4} + \frac{\sigma^4\phi^3(\nu_4-3)}{(1-\phi)^2}, & \text{if } \phi < 1, \\ \frac{2\sigma^4\phi^5}{(\phi-1)^4} + \frac{\sigma^4\phi^3(\nu_4-3)}{(\phi-1)^2}, & \text{if } \phi > 1. \end{cases}$$

Comparing the asymptotic variance σ_S^2 of $R_{(S,X)}(\widehat{\beta}^S; \beta)$ with optimal sketching and that of $R_{(S,X)}(\widehat{\beta}; \beta)$ without sketching, we have following observations. First, the non-trivial and optimal sketching in case (a) may result in a smaller asymptotic variance σ_S^2 than that for the full-sample estimator. Take standard Gaussian features with $\phi > 1$, for which the forth (central) moment ν_4 is 3, as an example. Then it can be verified that $\sigma_S^2 \leq 2\sigma^4\phi^3(\phi-1)^{-4} =: \sigma_0^2$ for $\phi \in (1, \alpha(\alpha-\sigma)^{-1})$ and $\sigma_S^2 \leq \sigma^4(2\phi-1)(1-\phi)^{-4}/8 < \sigma_0^2$ for $\phi \in (1-\sigma\alpha^{-1}/2, 1]$ when $\text{SNR} > 1$. Second, the trivial sketching in case (b) has a zero limiting variance because in this case the null estimator $\tilde{\beta} = 0$ is optimal.

CLTs for $R_{(\beta,S,X)}(\widehat{\beta}^S; \beta)$. In the underparameterized regime, for sufficiently large n , $B_{(\beta,S,X)}(\widehat{\beta}^S; \beta) \sim B_{(S,X)}(\widehat{\beta}^S; \beta) \sim 0$, and $V_{(\beta,S,X)}(\widehat{\beta}^S; \beta) \sim V_{(S,X)}(\widehat{\beta}^S; \beta)$. Thus, $B_{(\beta,S,X)}(\widehat{\beta}^S; \beta)$ has exactly the same CLT as $B_{(S,X)}(\widehat{\beta}^S; \beta)$ in Theorem [6.4](#). We now present the corresponding CLT in the overparameterized case.

Theorem 6.7. Assume Assumptions [2.3](#), [2.4](#), [6.3](#) and $\Sigma = I_p$. Suppose $\phi\psi^{-1} > 1$ and S is any sketching matrix S that satisfies Assumption [2.6](#). Then it holds that

$$\sqrt{p} \left(R_{(\beta,S,X)}(\widehat{\beta}^S; \beta) - \alpha^2(1 - \psi_n\phi_n^{-1}) - \frac{\sigma^2}{\phi_n\psi_n^{-1} - 1} \right) \xrightarrow{D} \mathcal{N}(\mu_3, \sigma_3^2),$$

where

$$\mu_3 = 0, \quad \sigma_3^2 = 2(1 - \phi^{-1}\psi)\alpha^4.$$

More precise versions of μ_3 and σ_3^2 are

$$\begin{aligned} \tilde{\mu}_3 &= \frac{1}{\sqrt{p}} \left(\frac{\sigma^2\phi\psi^{-1}}{(\phi\psi^{-1} - 1)^2} + \frac{\sigma^2(\nu_4 - 3)}{\phi\psi^{-1} - 1} \right), \\ \tilde{\sigma}_3^2 &= 2(1 - \phi^{-1}\psi)\alpha^4 + \frac{1}{p} \left(\frac{2\sigma^4\phi^3\psi^{-3}}{(\phi\psi^{-1} - 1)^4} + \frac{\sigma^4\phi\psi^{-1}(\nu_4 - 3)}{(\phi\psi^{-1} - 1)^2} \right). \end{aligned}$$

6.3 Misspecified model

This subsection briefly discusses the misspecified model. When the misspecification error, aka model bias, is included, the risk will decrease at first and then increase for the full-sample ridgeless least square estimator in the underparameterized case. This aligns with the classic statistical idea of “underfitting” and “overfitting”. This subsection studies the effect of sketching on the selection of the optimal sketching size.

We consider a misspecified in which we observe only a subset of the features. A similar model is also discussed in the section 5.1 of [Hastie et al. \(2022\)](#). Suppose the true model is

$$y_i = \beta^T x_i + \theta^T w_i + \varepsilon_i, \quad i = 1, \dots, n \quad (6.5)$$

where $x_i \in \mathbb{R}^p, w_i \in \mathbb{R}^q$ and the noise ε_i is independent of (x_i, w_i) . Further assume (x_i, w_i) are jointly Gaussian with mean zero and covariance matrix

$$\Sigma = \begin{bmatrix} \Sigma_{xx}, \Sigma_{xw} \\ \Sigma_{xw}^T, \Sigma_{ww} \end{bmatrix}.$$

We can only observe the data matrix $X = (x_1, \dots, x_n)^T \in \mathbb{R}^{n \times p}$. Still, we use the sketched data $\tilde{Y} := SY \in \mathbb{R}^m, \tilde{X} := SX \in \mathbb{R}^{m \times p}$ and its corresponding minimum-norm least square estimator $\tilde{\beta}^S$ defined in (1.2). Let $(x_{\text{new}}, w_{\text{new}})$ be a test point. The out-of-sample prediction risk is defined as

$$R_{(S, X)}(\tilde{\beta}^S; \beta, \theta) = \mathbb{E} \left[(x_{\text{new}}^T \tilde{\beta}^S - x_{\text{new}}^T \beta - w_{\text{new}}^T \theta)^2 \mid S, X \right].$$

Here we let β and θ are nonrandom parameters and the expectation is taken over $x_{\text{new}}, w_{\text{new}}, \varepsilon$ and also $W = (w_1, \dots, w_n)^T \in \mathbb{R}^{n \times q}$. Similar to lemma 2 in [Hastie et al. \(2022\)](#), we can decompose the risk into two terms,

$$R_{(S, X)}(\tilde{\beta}^S; \beta, \theta) = \underbrace{\mathbb{E} \left[(x_{\text{new}}^T \tilde{\beta}^S - \mathbb{E}(y_{\text{new}}|x_{\text{new}}))^2 \mid S, X \right]}_{R_{(S, X)}^*(\tilde{\beta}^S; \beta, \theta)} + \underbrace{\mathbb{E} \left[(\mathbb{E}(y_{\text{new}}|x_{\text{new}}) - \mathbb{E}(y_{\text{new}}|x_{\text{new}}, w_{\text{new}}))^2 \right]}_{M(\beta, \theta)},$$

where $M(\beta, \theta)$ can be seen as the misspecification bias. Notice that conditioning on x_i , model (6.5) is equivalent to $y_i = \tilde{\beta}^T x_i + \tilde{\varepsilon}_i$ where $\tilde{\beta} = \beta + \Sigma_{xx}^{-1} \Sigma_{xw} \theta$ and $\tilde{\varepsilon}_i \sim N(0, \tilde{\sigma}^2)$ is independent of x_i , $\tilde{\sigma}^2 = \sigma^2 + \theta^T \Sigma_{w|x} \theta$. Here $\Sigma_{w|x}$ is the covariance matrix of w_i given x_i , i.e., $\Sigma_{w|x} = \Sigma_{ww} - \Sigma_{xw}^T \Sigma_{xx}^{-1} \Sigma_{xw}$. Moreover, simple calculation shows $M(\beta, \theta) = \theta^T \Sigma_{w|x} \theta$. We refer readers to Remark 2 in [Hastie et al. \(2022\)](#) for more details.

We conclude that even for this misspecified model, since $M(\beta, \theta)$ is independent of the sketching matrix S , and $R_{(S, X)}^*(\tilde{\beta}^S; \beta, \theta)$ can still be approximated using Theorem 6.2, random sketching cannot improve the limiting risks by sketching the estimator to the underparameterized regime. We expect in more complicated models, for example, the random feature model in [Mei & Montanari \(2022\)](#), sketching to the underparameterized regime might help reduce the limiting risks. We leave this problem to the future.

7 Conclusions and Discussions

This paper studies the statistical role of downsampling for linear regression estimators, where downsampling is carried out by random sketching, and highlights a few interesting phenomena. Particularly, downsampling might actually help improve the generalization performance, which also inspires a practical procedure for constructing a stable sketched estimator. Our practical procedure requires the use of an additional validation dataset. A possible direction for future work is to refine this practical procedure with provable guarantees. Moreover, we hypothesis that Assumption 2.6 on the sketching matrix can be further relaxed. Currently, it excludes cases such as subsampling with replacement or Boosting by requiring the LSD of SS^\top to be away from zero. Another interesting direction is to establish central limit theorems for more general cases, for example, for i.i.d. sketching and correlated features.

References

Ailon, N. and Chazelle, B. Approximate nearest neighbors and the fast johnson-lindenstrauss transform. In *Proceedings of the thirty-eighth annual ACM symposium on Theory of computing*, pp. 557–563, 2006.

Ba, J., Erdogdu, M., Suzuki, T., Wu, D., and Zhang, T. Generalization of two-layer neural networks: An asymptotic viewpoint. In *Proceedings of the seventh International Conference on Learning Representations*, 2019.

Bai, Z. and Silverstein, J. W. No eigenvalues outside the support of the limiting spectral distribution of large-dimensional sample covariance matrices. *The Annals of Probability*, 26(1):316–345, 1998.

Bai, Z. and Silverstein, J. W. *Spectral Analysis of Large Dimensional Random Matrices*. Springer, New York, 2010.

Bai, Z. and Yao, J. Central limit theorems for eigenvalues in a spiked population model. *Annales de l'IHP Probabilités et Statistiques*, 44(3):447–474, 2008.

Bartlett, P. L., Long, P. M., Lugosi, G., and Tsigler, A. Benign overfitting in linear regression. *Proceedings of the National Academy of Sciences*, 117(48):30063–30070, 2020.

Belkin, M., Hsu, D., Ma, S., and Mandal, S. Reconciling modern machine learning practice and the bias-variance trade-off. *arXiv preprint arXiv:1812.11118*, 2018.

Canziani, A., Paszke, A., and Culurciello, E. An analysis of deep neural network models for practical applications. *arXiv preprint arXiv:1605.07678*, 2016.

Chatterji, N. S. and Long, P. M. Finite-sample analysis of interpolating linear classifiers in the overparameterized regime. *Journal of Machine Learning Research*, 22(1):5721–5750, 2021.

Couillet, R. and Hachem, W. Analysis of the limiting spectral measure of large random matrices of the separable covariance type. *Random Matrices: Theory and Applications*, 3(04):1450016, 2014.

Couillet, R. and Liao, Z. *Random Matrix Methods for Machine Learning*. Cambridge University Press, Cambridge, 2022.

Dobriban, E. and Liu, S. Asymptotics for sketching in least squares regression. *arXiv preprint arXiv:1810.06089*, 2018.

Dobriban, E. and Wager, S. High-dimensional asymptotics of prediction: ridge regression and classification. *The Annals of Statistics*, 46(1):247–279, 2018.

Drineas, P. and Mahoney, M. W. Lectures on randomized numerical linear algebra. *The Mathematics of Data*, 25(1), 2018.

El Karoui, N. Concentration of measure and spectra of random matrices: applications to correlation matrices, elliptical distributions and beyond. *The Annals of Applied Probability*, 19(6):2362–2405, 2009.

Golub, G. H. and Van Loan, C. F. *Matrix Computations*. Johns Hopkins University Press, Baltimore, 2013.

Gunasekar, S., Lee, J., Soudry, D., and Srebro, N. Characterizing implicit bias in terms of optimization geometry. In *Proceedings of the thirty-fifth International Conference on Machine Learning*, pp. 1832–1841. PMLR, 2018.

Hastie, T., Tibshirani, R., Friedman, J. H., and Friedman, J. H. *The Elements of Statistical Learning: Data Mining, Inference, and Prediction*. Springer, New York, 2009.

Hastie, T., Montanari, A., Rosset, S., and Tibshirani, R. J. Surprises in high-dimensional ridgeless least squares interpolation. *The Annals of Statistics*, 50(2):949–986, 2022.

He, K., Zhang, X., Ren, S., and Sun, J. Deep residual learning for image recognition. In *Proceedings of the twenty-ninth IEEE Conference on Computer Vision and Pattern Recognition*, pp. 770–778, 2016.

Knowles, A. and Yin, J. Anisotropic local laws for random matrices. *Probability Theory and Related Fields*, 169(1):257–352, 2017.

Li, Z., Xie, C., and Wang, Q. Asymptotic normality and confidence intervals for prediction risk of the min-norm least squares estimator. In *Proceedings of the thirty-eighth International Conference on Machine Learning*, pp. 6533–6542. PMLR, 2021.

Liang, T. and Rakhlin, A. Just interpolate: kernel “ridgeless” regression can generalize. *The Annals of Statistics*, 48(3):1329–1347, 2020.

Liang, T. and Recht, B. Interpolating classifiers make few mistakes. *arXiv preprint arXiv:2101.11815*, 2021.

Mahoney, M. W. Randomized algorithms for matrices and data. *Foundations and Trends in Machine Learning*, 3(2):123–224, 2011.

Marcenko, V. A. and Pastur, L. A. Distribution of eigenvalues for some sets of random matrices. *Mathematics of the USSR-Sbornik*, 1(4):457, 1967.

Mei, S. and Montanari, A. The generalization error of random features regression: Precise asymptotics and the double descent curve. *Communications on Pure and Applied Mathematics*, 75(4):667–766, 2022.

Mezzadri, F. How to generate random matrices from the classical compact groups. *arXiv preprint math-ph/0609050*, 2006.

Muthukumar, V., Narang, A., Subramanian, V., Belkin, M., Hsu, D., and Sahai, A. Classification vs regression in overparameterized regimes: Does the loss function matter? *Journal of Machine Learning Research*, 22(1):10104–10172, 2021.

Nakkiran, P., Kaplun, G., Bansal, Y., Yang, T., Barak, B., and Sutskever, I. Deep double descent: Where bigger models and more data hurt. *Journal of Statistical Mechanics: Theory and Experiment*, 2021(12):124003, 2021.

Neyshabur, B., Tomioka, R., and Srebro, N. In search of the real inductive bias: on the role of implicit regularization in deep learning. *arXiv preprint arXiv:1412.6614*, 2014.

Novak, R., Bahri, Y., Abolafia, D. A., Pennington, J., and Sohl-Dickstein, J. Sensitivity and generalization in neural networks: an empirical study. *arXiv preprint arXiv:1802.08760*, 2018.

Paul, D. and Silverstein, J. W. No eigenvalues outside the support of the limiting empirical spectral distribution of a separable covariance matrix. *Journal of Multivariate Analysis*, 100(1):37–57, 2009.

Pilanci, M. *Fast Randomized Algorithms for Convex Optimization and Statistical Estimation*. PhD thesis, University of California, Berkeley, 2016.

Raskutti, G. and Mahoney, M. W. A statistical perspective on randomized sketching for ordinary least-squares. *Journal of Machine Learning Research*, 17(1):7508–7538, 2016.

Richards, D., Mourtada, J., and Rosasco, L. Asymptotics of ridge (less) regression under general source condition. In *Proceedings of the twenty-fourth International Conference on Artificial Intelligence and Statistics*, pp. 3889–3897. PMLR, 2021.

Woodruff, D. P. Sketching as a tool for numerical linear algebra. *Foundations and Trends in Theoretical Computer Science*, 10(1–2):1–157, 2014.

Yao, J., Zheng, S., and Bai, Z. *Sample Covariance Matrices and High-Dimensional Data Analysis*. Cambridge University Press, Cambridge, 2015.

Zhang, C., Bengio, S., Hardt, M., Recht, B., and Vinyals, O. Understanding deep learning (still) requires rethinking generalization. *Communications of the ACM*, 64(3):107–115, 2021.

Zhang, L. *Spectral Analysis of Large Dimensional Random Matrices*. PhD thesis, National University of Singapore, Singapore, 2007.

Zheng, S., Bai, Z., and Yao, J. Substitution principle for clt of linear spectral statistics of high-dimensional sample covariance matrices with applications to hypothesis testing. *The Annals of Statistics*, 43(2):546–591, 2015.

Appendix

Overview We present the details on numerical studies in Section A. Sections B and C present the proofs for results with isotropic and correlated features respectively. We collect the proof of Theorem 6.2 in Section D and the proofs for results on CLTs in Section E.

A Details on numerical studies

A.1 Numerical studies for isotropic features

This section provides additional details on the numerical studies for isotropic features to replicate Figures 2 and 3.

A.1.1 Figure 2

For Figure 2, numerical simulations were run 500 replications. For each replication, we generated $\beta \sim \mathcal{N}_p\left(0, \frac{\alpha^2}{p} I_p\right)$ and a training dataset (X, Y) with $n = 400$ training samples, and a testing dataset $\{(x_{\text{new},i}, y_{\text{new},i}) : 1 \leq i \leq n_{\text{new}}\}$ with $n_{\text{new}} = 100$ testing samples. The feature, orthogonal sketching, and i.i.d. sketching matrices were generated and then fixed across all replications. The orthogonal matrix was generated using the function `ortho_group` from the Python library SciPy, while the feature matrix and i.i.d. sketching matrices were generated using Python library NumPy. Other details are given in the caption of Figure 2.

The finite-sample risks, aka the dots and crosses in Figure 2, were calculated as functions of ψ . Specifically, given fixed n , we varied ψ by taking a grid of $\psi \in (0, 1)$ with $|\psi_i - \psi_{i+1}| = \delta$ for $\delta = 0.05$. This led to a grid of values for m , i.e., $m_i = [\psi_i n]$. For each replication k , we randomly generated a coefficient vector $\beta(k)$. For each replication k , we first randomly generated a coefficient vector $\beta(k)$. Within replication k and for each m_i , we fitted a sketched ridgeless least square estimator $\widehat{\beta}(k)^{S_{m_i}}$ using the training dataset and calculated the empirical risks on the testing dataset:

$$\widehat{R}_{(S_{m_i}, X)}(\widehat{\beta}^{S_{m_i}}; \beta) = \frac{1}{500} \sum_{k=1}^{500} \left\{ \frac{1}{n_{\text{new}}} \sum_{r=1}^{n_{\text{new}}} (x_{\text{new},r}^T \widehat{\beta}(k)^{S_{m_i}} - x_{\text{new},r}^T \beta(k))^2 \right\}. \quad (\text{A.1})$$

A.1.2 Figure 3

The finite-sample risks, aka the dots in Figure 3, were calculated as functions of ϕ . Numerical simulation procedure and data generation followed Section A.1.1. The optimal sketching size m^* was selected based on Theorem 3.3. If $m^* = n$, we fitted a ridgeless least square estimator $\widehat{\beta}$ on the training set; if $m^* < n$, we fitted a sketched estimator $\widehat{\beta}^S$ with m^* . The empirical risks $\widehat{R}_{(S, X)}(\widehat{\beta}^S; \beta)$ were evaluated on the testing dataset in a similar way as in Equation (A.1). To indicate how SNR and ϕ influence the selection of m^* , the left panel of Figure 3 presents risks for $\text{SNR} < 1$, and the right panel presents risks for $\text{SNR} > 1$.

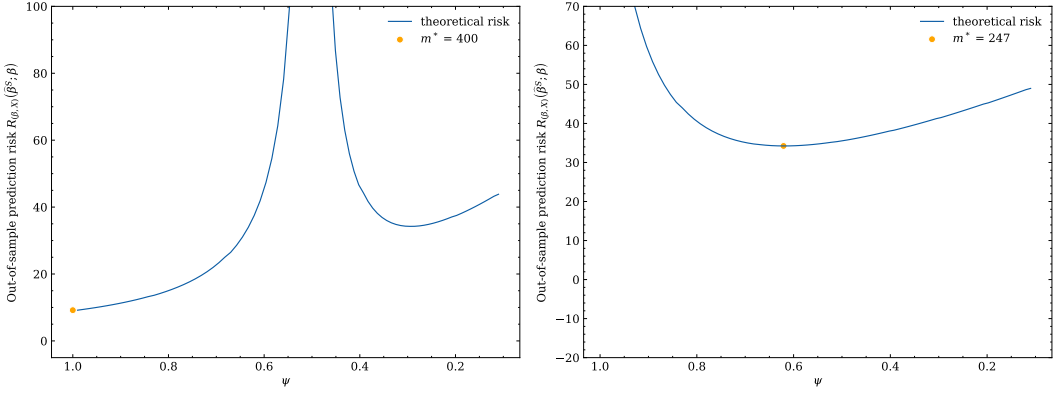


Figure 7: Asymptotic risk curves for sketched ridgeless least square estimators with correlated features, orthogonal sketching, as functions of ψ . The lines are theoretical risk curves for $n = 400$ with $p = 200$ and $p = 424$ respectively, where $\text{SNR} = \alpha/\sigma = 2$ with $(\alpha, \sigma) = (6, 3)$, ψ varying in $(0, 1)$, and $m = [n\psi]$. The dot marks the minimum of a theoretical risk curve within $\psi \in (0, 1)$.

A.2 Numerical studies for correlated features

This section provides additional details on numerical studies for correlated features to replicate Figures 4 and 5.

A.2.1 Figure 4

The numerical simulation procedure followed Section A.1.1. Instead of isotropic features, we generated correlated features. Other details are given in the caption of Figure 4.

A.2.2 Figure 5

The simulation procedure followed Section A.1.2 and the data generation followed Section A.2.1. In the case of correlated features, the theoretically optimal sketching size m^* does not have a closed-form representation, and m^* can be picked by minimizing the theoretical risk function across a set of values for m . Specifically, given fixed p and n , we varied ψ by taking a grid of $\psi \in (0, 1)$ with $|\psi_i - \psi_{i+1}| = \delta$ for $\delta = 0.05$. This led to a set of potential values for m^* , i.e., $m_i = [\psi_i n]$. For each m_i , we calculated the negative solutions c_0 in (4.1) and (4.4) numerically using the function `fsolve` in the Python library SciPy. These values of c_0 were then used to generate the theoretical risk curves in the overparameterized and underparameterized regime as described in Theorem 4.2 and Theorem 4.3, respectively. The optimal sketching size m^* was selected as the one that minimized the theoretical risks across all m_i . With the optimal sketching size m^* , the empirical risks were calculated the same way as in Section A.1.2.

We further illustrate how the sketching size was selected using two examples shown in Figure 7. For $p = 200$ in the left panel, the risk attained minimum at $\psi \approx 1$ and $m^* = 400$,

so no sketching was needed. For $p = 424$ in the right panel, the risk attained minimum at $\psi \approx 0.6175$ and we set $m^* = 0.6175 \times 400 = 247$.

B Proofs for isotropic features

B.1 Proof of Lemma 3.1

Because

$$\mathbb{E}(\widehat{\beta}^S | \beta, S, X) = (X^T S^T S X)^+ X^T S^T S X \beta,$$

$$\text{Cov}(\widehat{\beta}^S | \beta, S, X) = \sigma^2 (X^T S^T S X)^+ X^T S^T S S^T S X (X^T S^T S X)^+,$$

we can derive the expressions of $B_{(\beta, S, X)}(\widehat{\beta}^S; \beta)$, $V_{(\beta, S, X)}(\widehat{\beta}^S; \beta)$ and $V_{(S, X)}(\widehat{\beta}^S; \beta)$ from their respective definitions. $B_{(S, X)}(\widehat{\beta}^S; \beta)$ expression follows from the formula of the expectation of quadratic form and the fact that $(X^T S^T S X)^+ X^T S^T S X$ is idempotent.

Now since the eigenvalues of $I_p - (X^T S^T S X)^+ X^T S^T S X$ are either 0 or 1, the eigenvalues of $[(X^T S^T S X)^+ X^T S^T S X - I_p] \Sigma [(X^T S^T S X)^+ X^T S^T S X - I_p]$ are uniformly bounded over $[0, C_1]$. Then (3.1) can be obtained by applying (Bai & Silverstein, 2010, Lemma B.26).

B.2 Proof of Theorem 3.2

The proof for the underparameterized case directly follows from the Corollary 4.4 since the bias vanishes. As for the overparameterized case, according to Theorem 4.2, when $\Sigma = I_p$, a simple calculation shows $c_0 = \psi\phi^{-1} - 1$, and $B_{(S, X)}(\widehat{\beta}^S; \beta) \rightarrow \alpha^2(1 - \psi\phi^{-1})$, $V_{(S, X)}(\widehat{\beta}^S; \beta) \rightarrow \sigma^2(\psi\phi^{-1} - 1)^{-1}$, which then leads to the desired results. We collect the proofs for Corollary 4.4 and Theorem 4.2 in Sections C.2.2 and C.1.2 respectively.

B.3 Proof of Theorem 3.3

We prove this theorem for orthogonal and i.i.d. sketching separately. We start with orthogonal sketching.

Orthogonal sketching We start with orthogonal sketching first. Let

$$f(x) = \alpha^2(1 - x^{-1}) + \frac{\sigma^2}{x - 1}, \quad x > 1.$$

According to Theorem 3.2, for orthogonal sketching, both limiting risks in the overparameterized regime are $f(\phi\psi^{-1})$.

For the case of $\alpha \leq \sigma$, i.e., $\text{SNR} \leq 1$,

$$f'(x) = \alpha^2 x^{-2} - \frac{\sigma^2}{(x - 1)^2} = \frac{(\alpha^2 - \sigma^2)x^2 - 2\alpha^2 x + \alpha^2}{x^2(x - 1)^2} < 0, \quad \forall x > 1,$$

and $\lim_{x \rightarrow \infty} f(x) = \alpha^2$. Thus, if $\phi \geq 1$, $f(\phi\psi^{-1})$ decreases as ψ decreases. If $\phi < 1$, the limiting risks without sketching ($\psi = 1$) are $\frac{\sigma^2\phi}{1-\phi}$, which exceeds α^2 if and only if $\phi > \frac{\alpha^2}{\alpha^2 + \sigma^2}$. So the optimal sketching size is $m^* \ll n$ if $\phi > \frac{\alpha^2}{\alpha^2 + \sigma^2}$, and $m^* = n$ otherwise.

For the case of $\alpha > \sigma$, i.e., $\text{SNR} > 1$, $f(x)$ decreases when $x \in (1, \frac{\alpha}{\alpha-\sigma})$, and increases when $x \in [\frac{\alpha}{\alpha-\sigma}, \infty)$, and $f(\frac{\alpha}{\alpha-\sigma}) = \sigma(2\alpha - \sigma)$. Thus, if $\frac{\alpha}{\alpha-\sigma} \geq \phi > 1$, orthogonal sketching can help reduce the limiting risks to $\min_{x>1} f(x)$. If $\phi < 1$, the same improvement holds if and only if $\frac{\sigma^2\phi}{1-\phi} > \sigma(2\alpha - \sigma)$, or equivalently $\phi > 1 - \frac{\sigma}{2\alpha}$. Thus, the optimal sketching size is $m^* = \phi \frac{\alpha-\sigma}{\alpha} \cdot n = \frac{\alpha-\sigma}{\alpha} \cdot p$ if $1 - \frac{\sigma}{2\alpha} < \phi \leq \frac{\alpha}{\alpha-\sigma}$; and $m^* = n$ otherwise.

i.i.d. sketching Because in the underparameterized case, sketching always increases the risk which follows the classic statistical intuition: a larger sample size is better. In other words, only sketching to the overparameterized case can help reduce the risk. Because i.i.d. sketching shares the same limiting risks with orthogonal sketching in the overparameterized regime, it has the same optimal sketching size.

C Proofs for correlated features

C.1 Proofs for the over-parameterized case

C.1.1 Proof of Lemma 4.1

Let $f(c) = 1 - \int \frac{x}{-c+x\psi\phi^{-1}} dH(x)$. Because $f(0) = 1 - \phi\psi^{-1} < 0$, $f(-\infty) = 1$, and f is smooth, f has at least one negative root. Suppose c_1 and c_2 are two negative roots with $c_1 < c_2$. Then we have

$$0 = f(c_1) - f(c_2) = \int \frac{x(c_2 - c_1)}{(-c_2 + x\psi\phi^{-1})(-c_1 + x\psi\phi^{-1})} dH(x) > 0,$$

where the last inequality follows from the fact that the numerator and denominator are both larger than 0. This is a contradiction and thus f has a unique negative root.

C.1.2 Proof of Theorem 4.2

Bias part To prove the bias part (4.2), we first need some lemmas. Lemmas C.1 and C.2 show that the minimal nonzero eigenvalues of corresponding matrices are lower bounded, which will be used to guarantee to exchange limits. Lemma C.1 also proves, in the overparameterized case, $\frac{1}{p}SZZ^TS^T$ is invertible almost surely for all large n .

Lemma C.1. Let $Z \in \mathbb{R}^{n \times p}$ be a matrix with i.i.d. entries Z_{ij} such that $\mathbb{E}[Z_{ij}] = 0$, $\mathbb{E}[Z_{ij}^2] = 1$, and $\mathbb{E}[Z_{ij}^4] < \infty$. Assume Assumption 2.6 and suppose $m, n, p \rightarrow \infty$ such that $p/n \rightarrow \phi$, $m/n \rightarrow \psi \in (0, 1)$. Then, there exists some constant $\tau > 0$ such that almost surely for all large n , it holds that $\lambda_{\min}^+ \left(\frac{1}{p}SZZ^TS^T \right) = \lambda_{\min}^+ \left(\frac{1}{p}Z^TS^TSZ \right) \geq \tau$, where λ_{\min}^+ denotes the smallest nonzero eigenvalue. Furthermore, if (i) $\phi\psi^{-1} > 1$, then almost surely for all large n , $\frac{1}{p}SZZ^TS^T$ is invertible; (2) $\phi\psi^{-1} < 1$, then almost surely for all large n , $\frac{1}{p}Z^TS^TSZ$ is invertible.

Proof of Lemma C.1. Denote the limiting spectral measure of $\frac{1}{p}Z^TS^TSZ$ by μ . By (Yao et al., 2015, Proposition 2.17), the support of μ is completely determined by $\Psi(\alpha)$, known as

the functional inverse of the function $a(x) := -1/s(x)$, where $s(x)$ is the Stieltjes transform of μ . Specifically, if we let Γ be the support of μ , then $\Gamma^c \cap (0, \infty) = \{\Psi(a) : \Psi'(a) > 0\}$. Under Assumption 2.6, we can assume that the ESD of $S^T S$ converges to a nonrandom measure \underline{B} , which is the companion of B . Then, $\Psi(a) = a + \phi^{-1} a \int \frac{t}{a-t} d\underline{B}(t)$, and hence $\Psi'(a) = 1 + \phi^{-1} \int \frac{t}{a-t} d\underline{B}(t) - \phi^{-1} a \int \frac{t}{(a-t)^2} d\underline{B}(t)$, which is smooth.

(i) If $\phi^{-1}\psi < 1$, then $\lim_{a \rightarrow 0^+} \Psi'(a) = 1 - \phi^{-1}(1 - \underline{B}(\{0\})) = 1 - \phi^{-1}\psi > 0$. Thus, there exists some small enough $\epsilon > 0$ such that Ψ is increasing on $(0, \epsilon)$. Besides, under Assumption 2.6, the support of \underline{B} is a subset of $\{0\} \cup [\widetilde{C}_0, \widetilde{C}_1]$. Thus, when ϵ is small enough, Ψ is well defined on $(0, \epsilon)$. Since $\lim_{a \rightarrow 0^+} \Psi(a) = 0$ and Ψ' is smooth, we know that there exists some $\tau > 0$ such that $\{\Psi(a) : \Psi'(a) > 0\} \supseteq (0, \tau)$.

(ii) If $\phi^{-1}\psi > 1$, then $\lim_{a \rightarrow 0^-} \Psi'(a) < 0$, and hence we can find some small enough ϵ such that Ψ is decreasing on $(-\epsilon, 0)$. Since $\lim_{a \rightarrow -\infty} \Psi(a) = -\infty$, and by the smoothness of Ψ , we know $\{\Psi(a) : \Psi'(a) > 0\} \supseteq (0, \Psi(-\epsilon))$. Overall, by combining these two situations and using (Bai & Silverstein, 1998, Theorem 1.1), we can show that there exists some $\tau > 0$ such that almost surely for all large n , $\lambda_{\min}^+(\frac{1}{p}Z^T S^T S Z) \geq \tau$.

To prove the invertibility of $\frac{1}{p}S^T S^T S^T$ when $\phi\psi^{-1} > 1$, we first denote the limiting spectral measure of $\frac{1}{p}S^T S^T S^T$ by $\underline{\mu}$. With (Couillet & Hachem, 2014, Proposition 2.2), it holds that $\underline{\mu}(\{0\}) = 1 - \min\{1 - B(\{0\}), \frac{n}{m} \min\{\frac{p}{n}, 1\}\} = 0$ since $B(\{0\}) = 0$ under Assumption 2.6. We thus obtain the invertibility of $\frac{1}{p}S^T S^T S^T$ almost surely for all large n by using again (Bai & Silverstein, 1998, Theorem 1.1). When $\phi\psi^{-1} < 1$, the invertibility of $\frac{1}{p}Z^T S^T S Z$ follows from a similar argument. \square

Lemma C.2. Let $a, b > 0$ be two positive constants. Let $A \in \mathbb{R}^{n \times n}$ be a positive semidefinite matrix such that $\lambda_{\min}^+(A) \geq a$ and $\Sigma \in \mathbb{R}^{n \times n}$ a positive definite matrix such that $\lambda_{\min}(\Sigma) \geq b$. Then, $\lambda_{\min}^+(\Sigma^{1/2} A \Sigma^{1/2}) \geq ab$.

Proof of Lemma C.2. The result follows from

$$\begin{aligned} \lambda_{\min}^+(\Sigma^{1/2} A \Sigma^{1/2}) &\geq \min_{x \in \mathbb{R}^n : x^T \Sigma^{1/2} A \Sigma^{1/2} x \neq 0} \frac{x^T \Sigma^{1/2} A \Sigma^{1/2} x}{\|x\|^2} \\ &\geq \min_{x \in \mathbb{R}^n : x^T \Sigma^{1/2} A \Sigma^{1/2} x \neq 0} \frac{x^T \Sigma^{1/2} A \Sigma^{1/2} x}{\|\Sigma^{1/2} x\|^2} \cdot \min_{x \in \mathbb{R}^n : x \neq 0} \frac{\|\Sigma^{1/2} x\|^2}{\|x\|^2} \\ &= ab. \end{aligned}$$

\square

Lemma C.3. Assume Assumption 2.5 and suppose $\phi, \psi > 0$. Then for any $z < 0$, the following equation (C.1) has a unique negative solution $c(z) = c(z, \phi, \psi, H)$,

$$c(z) = \int \frac{(z + c(z))x}{-z - c(z) + x\psi\phi^{-1}} dH(x). \quad (\text{C.1})$$

Furthermore, $\lim_{z \rightarrow 0^-} c(z) = c_0$ where c_0 is defined by (4.1).

Proof of Lemma C.3. Given $z < 0$, let $f(c(z)) = c(z) - \int \frac{(z+c(z))x}{-z-c(z)+x\psi\phi^{-1}} dH(x)$. We have $f(-\infty) = -\infty$ and $f(0) = -\int \frac{zx}{-z+x\psi\phi^{-1}} dH(x) > 0$ since $z < 0$ and $x, \phi, \psi > 0$. By the smoothness of f , we know f has at least one negative solution. Suppose $c_1(z)$ and $c_2(z)$ are two negative solutions with $c_1(z) > c_2(z)$. Then, we have

$$\begin{aligned} 0 &= \int \frac{x(\frac{z}{c_1(z)} + 1)}{-z - c_1(z) + x\psi\phi^{-1}} dH(x) - \int \frac{x(\frac{z}{c_2(z)} + 1)}{-z - c_2(z) + x\psi\phi^{-1}} dH(x) \\ &= \int \left\{ \frac{x(c_1(z) - c_2(z))}{(-z - c_1(z) + x\psi\phi^{-1})(-z - c_2(z) + x\psi\phi^{-1})} + \frac{z^2 x(\frac{c_1(z) - c_2(z)}{c_1(z)c_2(z)})}{(-z - c_1(z) + x\psi\phi^{-1})(-z - c_2(z) + x\psi\phi^{-1})} \right. \\ &\quad \left. + \frac{zx^2\psi\phi^{-1}(\frac{c_2(z) - c_1(z)}{c_1(z)c_2(z)})}{(-z - c_1(z) + x\psi\phi^{-1})(-z - c_2(z) + x\psi\phi^{-1})} + \frac{zx(\frac{(c_1(z) - c_2(z))(c_1(z) + c_2(z))}{c_1(z)c_2(z)})}{(-z - c_1(z) + x\psi\phi^{-1})(-z - c_2(z) + x\psi\phi^{-1})} \right\} dH(x). \end{aligned}$$

Since $z, c_1(z), c_2(z) < 0$, it is easy to find that each term above is larger than 0. This contradiction shows for given $z < 0$, (C.1) has a unique negative solution, denoted by $c(z)$.

Next, we show $\lim_{z \rightarrow 0^-} c(z) = c_0$. Given $z < 0$, let

$$g(a, z) = 1 - \int \frac{x}{-z - a + x\psi\phi^{-1}} dH(x) - \int \frac{z/a}{-z - a + x\psi\phi^{-1}} dH(x).$$

Since $c(z)$ is the solution of (C.1), $g(c(z), z) = 0$. For any small $\epsilon > 0$, we can find a sufficiently small $\delta_1 > 0$ such that, when $-\delta_1 < z < 0$, we have $0 < -z - c_0 - \epsilon + x\psi\phi^{-1} < -c_0 + x\psi\phi^{-1}$. The second inequality is satisfied by taking $\delta_1 < \epsilon$. Because x lies in the support of the measure H , $x > C_0 > 0$. Moreover, since $c_0 < 0$, the first inequality holds when ϵ and δ_1 are sufficiently small. Because c_0 is the root of g when $z = 0$, in this case, we have $g(c_0 + \epsilon, z) < 0$ when $z \in (-\delta_1, 0)$. Furthermore, we can find a sufficiently small $\delta_2 > 0$ such that $g(c_0 - \epsilon, z) > 0$ when $z \in (-\delta_2, 0)$. This is because $g(c_0, 0) = 0$, $1 - \int \frac{x}{-c_0 + \epsilon + x\psi\phi^{-1}} dH(x) > 0$, and $\lim_{z \rightarrow 0^-} \int \frac{z/a}{-z - a + x\psi\phi^{-1}} dH(x) = 0$.

To conclude, taking $\delta = \min\{\delta_1, \delta_2\}$, we have, when $z \in (-\delta, 0)$, $g(c_0 + \epsilon, z) < 0$ and $g(c_0 - \epsilon, z) > 0$. By the smoothness of $g(a, z)$ with respect to a , we know $c(z) \in (c_0 - \epsilon, c_0 + \epsilon)$. Using the definition of a limit completes the proof. \square

Now we prove the bias part (4.2).

Proof of the bias part (4.2). For all large n , we have almost surely

$$\begin{aligned} &(X^T S^T S X)^+ X^T S^T S X \\ &= (S X)^+ S X \\ &= \lim_{\delta \rightarrow 0^+} X^T S^T (S X X^T S^T + \delta I_m)^{-1} S X \\ &= X^T S^T (S X X^T S^T)^{-1} S X, \end{aligned} \tag{C.2}$$

where the first equality uses $A^+ = (A^T A)^+ A^T$ for any matrix A , the second inequality uses $A^+ = \lim_{\delta \rightarrow 0^+} A^T (A A^T + \delta I)^{-1}$, and the third equality follows from Lemma C.1 and Assumption 2.5. Specifically, when $S Z Z^T S^T$ is invertible and Σ satisfies Assumption 2.5, then

$SXX^TS^T = SZ\Sigma Z^TS^T$ is also invertible. Let the singular value decomposition (SVD) of S be $S = UDV$ where $U \in \mathbb{R}^{m \times m}$, $V \in \mathbb{R}^{m \times n}$ are both orthogonal matrices, $D \in \mathbb{R}^{m \times m}$ is a diagonal matrix. By Assumption 2.6, we know almost surely for all large n , D is invertible. Then the RHS (right hand side) of (C.2) can be written as

$$X^TS^T(SXX^TS^T)^{-1}SX = X^TV^T(VXX^TV^T)^{-1}VX = (X^TV^TVX)^+X^TV^TVX. \quad (\text{C.3})$$

Thus, by (C.2), (C.3) and Lemma 3.1, we have

$$B_{(S,X)}(\widehat{\beta}^S; \beta) = \frac{\alpha^2}{p} \text{tr} \left\{ \left[I_p - \left(\frac{1}{p} X^TV^TVX \right)^+ \frac{1}{p} X^TV^TVX \right] \Sigma \right\}. \quad (\text{C.4})$$

For any $z < 0$,

$$\begin{aligned} & \left| \frac{1}{p} \text{tr} \left[\left(\frac{1}{p} X^TV^TVX \right)^+ \frac{1}{p} X^TV^TVX \Sigma \right] - \frac{1}{p} \text{tr} \left[\left(\frac{1}{p} X^TV^TVX - zI_p \right)^{-1} \frac{1}{p} X^TV^TVX \Sigma \right] \right| \\ & \leq \frac{|z| \|\Sigma\|_2}{\lambda_{\min}^+ \left(\frac{1}{p} X^TV^TVX \right) - z} \\ & = \frac{|z| \|\Sigma\|_2}{\lambda_{\min}^+ \left(\frac{1}{p} \Sigma^{1/2} Z^TV^TVZ\Sigma^{1/2} \right) - z} \leq \frac{|z| C_1}{C_0 \tau - z}, \end{aligned}$$

where the last inequality follows from Lemmas C.1, C.2 and Assumption 2.5. Thus, taking limits on both sides of (C.4) gives

$$\begin{aligned} \lim_{n \rightarrow \infty} B_{(S,X)}(\widehat{\beta}^S; \beta) &= \alpha^2 \lim_{n \rightarrow \infty} \lim_{z \rightarrow 0^-} \frac{1}{p} \text{tr} \left\{ \left[I_p - \left(\frac{1}{p} X^TV^TVX - zI_p \right)^{-1} \frac{1}{p} X^TV^TVX \right] \Sigma \right\} \\ &= \alpha^2 \lim_{n \rightarrow \infty} \lim_{z \rightarrow 0^-} \frac{1}{p} \text{tr} \left\{ \left[I_p - \left(\frac{1}{p} X^TV^TVX - zI_p \right)^{-1} \left(\frac{1}{p} X^TV^TVX - zI_p + zI_p \right) \right] \Sigma \right\} \\ &= -\alpha^2 \lim_{n \rightarrow \infty} \lim_{z \rightarrow 0^-} z \frac{1}{p} \text{tr} \left[\left(\frac{1}{p} X^TV^TVX - zI_p \right)^{-1} \Sigma \right]. \end{aligned} \quad (\text{C.5})$$

Now we can follow a similar argument to the proof of Theorem 1 in Hastie et al. (2022) to show the validity of exchanging the limits $n \rightarrow \infty$ and $z \rightarrow 0^-$. Define $f_n(z) = -\frac{z}{p} \text{tr} \left[\left(\frac{1}{p} X^TV^TVX - zI_p \right)^{-1} \Sigma \right]$. Since $|f_n(z)| \leq |z| \left\| \left(\frac{1}{p} X^TV^TVX - zI_p \right)^{-1} \right\|_2 \|\Sigma\|_2 \leq C_1$, we know $f_n(z)$ is uniformly bounded. Besides,

$$\begin{aligned} |f'_n(z)| &\leq \frac{1}{p} \left| \text{tr} \left[\left(\frac{1}{p} X^TV^TVX - zI_p \right)^{-1} \Sigma \right] + z \text{tr} \left[\left(\frac{1}{p} X^TV^TVX - zI_p \right)^{-2} \Sigma \right] \right| \\ &\leq \frac{\lambda_{\min}^+ \left(\frac{1}{p} X^TV^TVX \right) \|\Sigma\|_2}{\left[\lambda_{\min}^+ \left(\frac{1}{p} X^TV^TVX \right) - z \right]^2} \\ &\leq \frac{\|\Sigma\|_2}{\lambda_{\min}^+ \left(\frac{1}{p} X^TV^TVX \right)} \leq \frac{C_1}{C_0 \tau} \end{aligned} \quad (\text{C.6})$$

where the last inequality holds almost surely for all large n . As its derivatives are bounded, the sequence $\{f_n\}_{n=1}^\infty$ is equicontinuous, and hence, by the Arzela-Ascoli theorem, f_n converges uniformly. Thus, we can use Moore-Osgood theorem to conclude the validity of exchanging the limits $n \rightarrow \infty$ and $\lambda \rightarrow 0^-$. Define

$$m_{1n}(z) = \frac{1}{p} \text{tr} \left[\left(\frac{1}{p} \Sigma^{1/2} Z^T V^T V Z \Sigma^{1/2} - z I_p \right)^{-1} \Sigma \right], \quad m_{2n}(z) = \frac{1}{p} \text{tr} \left[\left(\frac{1}{p} V Z \Sigma Z^T V^T - z I_m \right)^{-1} \right]. \quad (\text{C.7})$$

According to [Zhang \(2007\)](#), almost surely, as $n \rightarrow \infty$, $m_{1n}(z) \rightarrow m_1(z)$, and $m_{2n}(z) \rightarrow m_2(z)$ where for given $z < 0$, $(m_1(z), m_2(z)) \in \mathbb{R}^+ \times \mathbb{R}^+$ is the unique solution of the self-consistent equations

$$\begin{aligned} m_1(z) &= \int \frac{x}{-z[1+xm_2(z)]} dH(x), \\ m_2(z) &= \psi \phi^{-1} \frac{1}{-z[1+m_1(z)]}. \end{aligned} \quad (\text{C.8})$$

Substituting m_2 into m_1 in (C.8) and multiplying both sides by z , we obtain

$$zm_1(z) = \int \frac{(z+zm_1(z))x}{-z-zm_1(z)+x\psi\phi^{-1}} dH(x).$$

By lemma [C.3](#), we know $\lim_{z \rightarrow 0^-} zm_1(z) = c_0$. Exchanging the limits in (C.5), we have almost surely

$$\begin{aligned} \lim_{n \rightarrow \infty} B_{(S,X)}(\widehat{\beta}^S; \beta) &= -\alpha^2 \lim_{z \rightarrow 0^-} \lim_{n \rightarrow \infty} z \frac{1}{p} \text{tr} \left[\left(\frac{1}{p} X^T V^T V X - z I_p \right)^{-1} \Sigma \right] \\ &= -\alpha^2 \lim_{z \rightarrow 0^-} zm_1(z) = -\alpha^2 c_0. \end{aligned}$$

Lemma [3.1](#) assures that $B_{(\beta,S,X)}(\widehat{\beta}^S; \beta)$ converges almost surely to the same limit. \square

Variance part To prove the variance part (4.3), we need the following theorem, often known as the Vitali's theorem ([Bai & Silverstein, 2010, Lemma 2.14](#)). This theorem ensures the convergence of the derivatives of converging analytic functions.

Lemma C.4 (Vitali's convergence theorem). Let f_1, f_2, \dots be analytic on the domain D , satisfying $|f_n(z)| \leq M$ for every n and $z \in D$. Suppose that there is an analytic function f on D such that $f_n(z) \rightarrow f(z)$ for all $z \in D$. Then it also holds that $f'_n(z) \rightarrow f'(z)$ for all $z \in D$.

Proof of the variance part (4.3). Let the singular value decomposition (SVD) of S be $S = UDV$ where $U \in \mathbb{R}^{m \times m}$, $V \in \mathbb{R}^{m \times n}$ are both orthogonal matrices, $D \in \mathbb{R}^{m \times m}$ is a diagonal matrix. According to Lemma [3.1](#),

$$\begin{aligned} V_{(S,X)}(\widehat{\beta}^S; \beta) &= \sigma^2 \text{tr} \left[(X^T S^T S X)^+ X^T S^T S S^T S X (X^T S^T S X)^+ \Sigma \right] \\ &= \sigma^2 \text{tr} \left[(S X)^+ S S^T (X^T S^T)^+ \Sigma \right] \end{aligned}$$

$$\begin{aligned}
&= \sigma^2 \text{tr} \left[\lim_{\delta \rightarrow 0^+} X^T S^T (S X X^T S^T + \delta I_m)^{-1} S S^T (S X X^T S^T + \delta I_m)^{-1} S X \Sigma \right] \\
&= \sigma^2 \text{tr} \left[X^T S^T (S X X^T S^T)^{-1} S S^T (S X X^T S^T)^{-1} S X \Sigma \right] \\
&= \sigma^2 \text{tr} \left[X^T V^T (V X X^T V^T)^{-2} V X \Sigma \right] \\
&= \sigma^2 \text{tr} \left[(V X)^+ (X^T V^T)^+ \Sigma \right] \\
&= \sigma^2 \text{tr} \left[(X^T V^T V X)^+ \Sigma \right] \\
&= \frac{\sigma^2}{p} \text{tr} \left[\left(\frac{1}{p} X^T V^T V X \right)^+ \Sigma \right], \tag{C.9}
\end{aligned}$$

where similar to the proof of the bias part in Theorem 3.2, we use the identity $A^+ = (A^T A)^+ A^T = \lim_{\delta \rightarrow 0^+} A^T (A A^T + \delta I)^{-1}$ for any matrix A , and the fact that almost surely for all large n , $S X X^T S^T$ is invertible. Define

$$g_n(z) = \frac{1}{p} \text{tr} \left[\left(\frac{1}{p} X^T V^T V X \right) \left(\frac{1}{p} X^T V^T V X - z I_p \right)^{-2} \Sigma \right].$$

Since for any $z \leq 0, x > 0$, we have

$$\left| \frac{x}{(x-z)^2} - \frac{1}{x} \right| \leq \frac{2|z|}{x^2}.$$

Thus, by Lemma C.2 and Assumption 2.5, for any $z < 0$,

$$\left| \frac{V_{(S,X)}(\widehat{\beta}^S; \beta)}{\sigma^2} - g_n(z) \right| \leq \frac{2|z|}{\left[\lambda_{\min}^+ \left(\frac{1}{p} X^T V^T V X \right) \right]^2} \|\Sigma\|_2 \leq \frac{2|z| C_1}{(C_0 \tau)^2}. \tag{C.10}$$

By (C.10), we can continue (C.9),

$$\begin{aligned}
&\lim_{n \rightarrow \infty} V_{(S,X)}(\widehat{\beta}^S; \beta) \\
&= \sigma^2 \lim_{n \rightarrow \infty} \lim_{z \rightarrow 0^-} \frac{1}{p} \text{tr} \left[\left(\frac{1}{p} X^T V^T V X \right) \left(\frac{1}{p} X^T V^T V X - z I_p \right)^{-2} \Sigma \right] \\
&= \sigma^2 \lim_{n \rightarrow \infty} \lim_{z \rightarrow 0^-} \frac{1}{p} \text{tr} \left[\left(\frac{1}{p} X^T V^T V X - z I_p + z I_p \right) \left(\frac{1}{p} X^T V^T V X - z I_p \right)^{-2} \Sigma \right] \\
&= \sigma^2 \lim_{n \rightarrow \infty} \lim_{z \rightarrow 0^-} \frac{1}{p} \text{tr} \left[\left(\frac{1}{p} X^T V^T V X - z I_p \right)^{-1} \Sigma + \frac{1}{p} \text{tr} \left[z \left(\frac{1}{p} X^T V^T V X - z I_p \right)^{-2} \Sigma \right] \right], \tag{C.11}
\end{aligned}$$

We now verify the validity of exchanging the limits $n \rightarrow \infty$ and $z \rightarrow 0^-$. As in the proof of the bias part of Theorem 3.2, in order to use Arzela-Ascoli theorem and Moore-Osgood theorem, it suffices to show $g_n(z)$ and $g'_n(z)$ are both uniformly bounded. We know it holds almost surely for all large n that for any $z < 0$,

$$|g_n(z)| \leq \frac{\left\| \frac{1}{p} X^T V^T V X \right\|_2 \|\Sigma\|_2}{\left[\lambda_{\min}^+ \left(\frac{1}{p} X^T V^T V X \right) - z \right]^2} \leq \frac{\left\| \frac{1}{p} Z Z^T \right\|_2 \|V^T V\|_2 \|\Sigma\|_2^2}{\left[\lambda_{\min}^+ \left(\frac{1}{p} X^T V^T V X \right) - z \right]^2} \leq \frac{(1 + \sqrt{\phi^{-1}})^2 C_1^2}{(C_0 \tau)^2}.$$

Moreover,

$$\begin{aligned} |g'_n(z)| &= \left| \frac{2}{p} \text{tr} \left[\left(\frac{1}{p} X^T V^T V X - z I_p \right)^{-2} \Sigma \right] + \frac{2}{p} \text{tr} \left[z \left(\frac{1}{p} X^T V^T V X - z I_p \right)^{-3} \Sigma \right] \right| \\ &\leq \frac{2 \left\| \frac{1}{p} X^T V^T V X \right\|_2 \|\Sigma\|_2}{\left[\lambda_{\min}^+ \left(\frac{1}{p} X^T V^T V X \right) - z \right]^3} \leq \frac{2 (1 + \sqrt{\phi^{-1}})^2 C_1^2}{(C_0 \tau)^3}. \end{aligned}$$

Thus, $g_n(z)$ and $g'_n(z)$ are both uniformly bounded and hence, we can exchange the limits. Recall the definition of $m_{1n}(z)$ in (C.7), we know $g_n(z) = m_{1n}(z) + zm'_{1n}(z) = (zm_{1n}(z))'$. We will use Lemma C.4 to show $g_n(z) \rightarrow m_1(z) + zm'_1(z)$ almost surely as $n \rightarrow \infty$. Since $zm_{1n}(z)$ and $zm_1(z)$ are analytic on $(-\infty, 0)$ such that $zm_{1n}(z) \rightarrow zm_1(z)$; see Zhang (2007). In addition, as in the proof of the bias part of Theorem 3.2, almost surely for all large n , it holds that $|zm_{1n}(z)| \leq C_1$. Thus the conditions of Lemma C.4 are satisfied. By exchanging the limits in (C.11) and using Lemma C.4, we obtain

$$\lim_{n \rightarrow \infty} V_{(S,X)}(\widehat{\beta}^S; \beta) = \sigma^2 \lim_{z \rightarrow 0^-} \lim_{n \rightarrow \infty} g_n(z) = \sigma^2 \lim_{z \rightarrow 0^-} m_1(z) + zm'_1(z). \quad (\text{C.12})$$

Recall the self-consistent equations in (C.8). A direct calculation yields

$$m_1(z) + zm'_1(z) = \int \frac{(1 + m_1(z) + zm'_1(z)) x^2 \psi \phi^{-1}}{(z + zm_1(z) - x \psi \phi^{-1})^2} dH(x).$$

Taking $z \rightarrow 0^-$ in the above equality and using $\lim_{z \rightarrow 0^-} zm_1(z) = c_0$ in Lemma C.3, we derive

$$\lim_{z \rightarrow 0^-} m_1(z) + zm'_1(z) = \frac{\int \frac{x^2 \psi \phi^{-1}}{(c_0 - x \psi \phi^{-1})^2} dH(x)}{1 - \int \frac{x^2 \psi \phi^{-1}}{(c_0 - x \psi \phi^{-1})^2} dH(x)}.$$

Combining the above limit with (C.12), we have almost surely

$$\lim_{n \rightarrow \infty} V_{(S,X)}(\widehat{\beta}^S; \beta) = \sigma^2 \frac{\int \frac{x^2 \psi \phi^{-1}}{(c_0 - x \psi \phi^{-1})^2} dH(x)}{1 - \int \frac{x^2 \psi \phi^{-1}}{(c_0 - x \psi \phi^{-1})^2} dH(x)}.$$

Lemma 3.1 assures that $V_{(\beta,S,X)}(\widehat{\beta}^S; \beta)$ converges almost surely to the same limit. \square

C.2 Proofs for the under-parameterized case

C.2.1 Proof of Theorem 4.3

According to Lemma C.1 and Assumption 2.5, we know almost surely for all large n , $\frac{1}{p} X^T S^T S X$ is invertible. Thus by Lemma 3.1, it holds that almost surely for all large n , $B_{(S,X)}(\widehat{\beta}^S; \beta) = B_{(\beta,S,X)}(\widehat{\beta}^S; \beta) = 0$ and hence (4.5) holds. To show the limiting variance (4.6), we follow from a similar proof to that for the bias part in Theorem 3.2. To be concise, we only sketch the proof here. Similar to (C.9) and (C.11), we have

$$V_{(S,X)}(\widehat{\beta}^S; \beta)$$

$$\begin{aligned}
&= \sigma^2 \text{tr} \left[(X^T S^T S X)^{-1} X^T S^T S S^T S X (X^T S^T S X)^{-1} \Sigma \right] \\
&= \sigma^2 \text{tr} \left[(Z^T S^T S Z)^{-1} Z^T S^T S S^T S Z (Z^T S^T S Z)^{-1} \right] \\
&= \sigma^2 \text{tr} \left[(Z^T S^T)^+ (S Z)^+ S S^T \right] \\
&= \sigma^2 \text{tr} \left[(S Z Z^T S^T)^+ S S^T \right] \\
&= \frac{\sigma^2}{n} \text{tr} \left[\left(\frac{1}{n} S Z Z^T S^T \right)^+ S S^T \right] \\
&= \sigma^2 \lim_{z \rightarrow 0^-} \frac{1}{n} \text{tr} \left[\left(\frac{1}{n} S Z Z^T S^T \right) \left(\frac{1}{n} S Z Z^T S^T - z I_m \right)^{-2} S S^T \right] \\
&= \sigma^2 \lim_{z \rightarrow 0^-} \frac{1}{n} \text{tr} \left[\left(\frac{1}{n} S Z Z^T S^T - z I_m \right)^{-1} S S^T \right] + \frac{1}{n} \text{tr} \left[z \left(\frac{1}{n} S Z Z^T S^T - z I_m \right)^{-2} S S^T \right]. \quad (\text{C.13})
\end{aligned}$$

Define

$$\tilde{m}_{1n}(z) = \frac{1}{n} \text{tr} \left[\left(\frac{1}{n} S Z Z^T S^T - z I_m \right)^{-1} S S^T \right], \quad \tilde{m}_{2n}(z) = \frac{1}{n} \text{tr} \left[\left(\frac{1}{n} Z^T S^T S Z - z I_p \right)^{-1} \right]. \quad (\text{C.14})$$

Then $\tilde{m}_{1n}(z) \rightarrow \tilde{m}_1(z)$ and $\tilde{m}_{2n}(z) \rightarrow \tilde{m}_2(z)$ almost surely as $n \rightarrow \infty$, where $(\tilde{m}_1(z), \tilde{m}_2(z)) \in \mathbb{R}^+ \times \mathbb{R}^+$ is the unique solution of the self-consistent equations (Zhang, 2007)

$$\begin{aligned}
\tilde{m}_1(z) &= \psi \int \frac{x}{-z[1+x\tilde{m}_2(z)]} dB(x), \\
\tilde{m}_2(z) &= \phi \frac{1}{-z[1+\tilde{m}_1(z)]}, \quad (\text{C.15})
\end{aligned}$$

for any $z < 0$. Substituting \tilde{m}_2 into \tilde{m}_1 in (C.15) and multiplying both sides by z , we obtain

$$z\tilde{m}_1(z) = \int \psi \frac{(z+z\tilde{m}_1(z))x}{-z-z\tilde{m}_1(z)+x\phi} dH(x).$$

Following the similar proofs to Lemma C.3 and the bias part in Theorem 3.2, we can obtain $\lim_{z \rightarrow 0^-} z\tilde{m}_1(z) = \tilde{c}_0$ where \tilde{c}_0 is defined in (4.4). Following the same argument for verifying interchange of the limits and Lemma C.4, we have

$$\begin{aligned}
\lim_{n \rightarrow \infty} V_{(S,X)}(\widehat{\beta}^S; \beta) &= \lim_{n \rightarrow \infty} V_{(\beta, S, X)}(\widehat{\beta}^S; \beta) \\
&= \sigma^2 \lim_{z \rightarrow 0^-} \tilde{m}_1(z) + z\tilde{m}'_1(z) = \sigma^2 \frac{\psi \int \frac{x^2 \phi}{(\tilde{c}_0 - x\phi)^2} dB(x)}{1 - \psi \int \frac{x^2 \phi}{(\tilde{c}_0 - x\phi)^2} dB(x)}.
\end{aligned}$$

C.2.2 Proof of Corollary 4.4

When S is an orthogonal sketching matrix, i.e., $S S^T = I_m$, we have $B(x) = \delta_{\{1\}}(x)$ where δ is the Dirac function. A simple calculation shows $\tilde{c}_0 = \phi - \psi$, and hence

$$V_{(S,X)}(\widehat{\beta}^S; \beta) = V_{(\beta, S, X)}(\widehat{\beta}^S; \beta) \rightarrow \sigma^2 \frac{\psi \int \frac{x^2 \phi}{(\tilde{c}_0 - x\phi)^2} dB(x)}{1 - \psi \int \frac{x^2 \phi}{(\tilde{c}_0 - x\phi)^2} dB(x)} = \sigma^2 \frac{\phi \psi^{-1}}{1 - \phi \psi^{-1}}.$$

When S is an i.i.d. sketching matrix, we know that almost surely, the ESD of SS^\top converges to the M-P law with parameter ψ , whose CDF (cumulative distribution function) is denoted by F_ψ , i.e., $B = F_\psi$. The self-consistent equation (4.4) reduces to

$$1 = \frac{\psi}{\phi} + \frac{\psi \tilde{c}_0}{\phi^2} s_\psi \left(\frac{\tilde{c}_0}{\phi} \right)$$

where s_ψ is the Stieltjes transform of M-P law with parameter ψ . According to the seminal work (Marcenko & Pastur, 1967), we know for any $z < 0$,

$$s_\psi(z) = \frac{1 - \psi - z - \sqrt{(z - 1 - \psi)^2 - 4\psi}}{c\psi z}.$$

A direct calculation shows $\tilde{c}_0 = -\psi - \phi^2 + \phi + \psi\phi$. Furthermore,

$$\begin{aligned} \psi \int \frac{x^2 \phi}{(\tilde{c}_0 - x\phi)^2} dB(x) &= \psi\phi^{-1} \int \frac{x^2}{(x - \tilde{c}_0\phi^{-1})^2} dF_\psi(x) \\ &= \psi\phi^{-1} \left[1 + 2\tilde{c}_0\phi^{-1} s_\psi(\tilde{c}_0\phi^{-1}) + (\tilde{c}_0\phi^{-1})^2 s'_\psi(\tilde{c}_0\phi^{-1}) \right] \\ &= \frac{\phi - 2\phi^2\psi^{-1} + \phi\psi^{-1}}{1 - \phi^2\psi^{-1}}. \end{aligned}$$

Plugging the above equality into (4.6), we get

$$V_{(S,X)}(\widehat{\beta}^S; \beta) = V_{(\beta, S, X)}(\widehat{\beta}^S; \beta) \rightarrow \sigma^2 \left(\frac{\phi}{1 - \phi} + \frac{\phi\psi^{-1}}{1 - \phi\psi^{-1}} \right).$$

C.2.3 Proof of Corollary 4.5

According to (4.4), we have

$$1 = \psi\phi^{-1} + \psi\tilde{c}_0\phi^{-2} \int \frac{1}{x - \tilde{c}_0\phi^{-1}} dB(x) = \psi\phi^{-1} (1 + ts_B(t)),$$

where $t = \tilde{c}_0\phi^{-1}$ and $s_B(z) = \int \frac{1}{x-z} dB(x)$ is the Stieltjes transform of the measure B . Thus, we have $ts_B(t) = \psi^{-1}\phi - 1$. In order to minimize (4.6), it suffices to minimize the numerator $\psi\phi^{-1} \int \frac{x^2}{(t-x)^2} dB(x)$, which after simplification is $\psi\phi^{-1} [1 + 2ts_B(t) + t^2 s'_B(t)]$. Therefore it suffices to minimize $t^2 s'_B(t)$. By the Cauchy-Schwartz inequality, we have

$$t^2 s'_B(t) = \int \frac{t^2}{(x-t)^2} dB(x) \geq \left(\int \frac{t}{x-t} dB(x) \right)^2 = (\psi^{-1}\phi - 1)^2,$$

and the minimum is achieved at $B = \delta_{\{a\}}$ ($a > 0$).

D Proof of Theorem 6.2

The proof to the variance part is the same as those for Theorem 4.2 and Theorem 4.3. As for the bias part, when $p/m \rightarrow \phi\psi^{-1} < 1$, same as (4.5), it is easy to show almost surely for all large n , $B_{(\beta, S, X)}(\widehat{\beta}^S; \beta) = 0$. Hence, we only need to prove the bias part (6.4) for

$p/m \rightarrow \phi\psi^{-1} > 1$. Without loss of generality, we assume $\|\beta\| = 1$ throughout the proof. Let the SVD of S be $S = UDV$ where $U \in \mathbb{R}^{m \times m}$, $V \in \mathbb{R}^{m \times n}$ are both orthogonal matrices, and $D \in \mathbb{R}^{m \times m}$ is a diagonal matrix. According to (C.2) and (C.3), we have

$$B_{(\beta, S, X)}(\widehat{\beta}^S; \beta) = \left\| \Sigma^{1/2} \left[(X^T V^T V X)^+ X^T V^T V X - I_p \right] \beta \right\|^2.$$

Let

$$h_n(z) = \left\| \Sigma^{1/2} \left[\left(\frac{1}{p} X^T V^T V X - z I_p \right)^{-1} \frac{1}{p} X^T V^T V X - I_p \right] \beta \right\|^2.$$

Then, for any $z < 0$,

$$\begin{aligned} & \left| B_{(\beta, S, X)}(\widehat{\beta}^S; \beta)^{1/2} - h_n(z)^{1/2} \right| \\ & \leq \left\| \Sigma^{1/2} \left[\left(\frac{1}{p} X^T V^T V X \right)^+ \frac{1}{p} X^T V^T V X - \left(\frac{1}{p} X^T V^T V X - z I_p \right)^{-1} \frac{1}{p} X^T V^T V X \right] \beta \right\| \\ & \leq \left\| \Sigma^{1/2} \right\|_2 \|\beta\| \frac{|z|}{\lambda_{\min}^+ \left(\frac{1}{p} X^T V^T V X \right) - z} \\ & \leq \frac{\sqrt{C_1} |z|}{\lambda_{\min}^+ \left(\frac{1}{p} X^T V^T V X \right) - z} \leq \frac{\sqrt{C_1} |z|}{C_0 \tau}, \end{aligned} \tag{D.1}$$

where the last inequality uses Lemma C.1 and C.2. By the fact that $|B_{(\beta, S, X)}(\widehat{\beta}^S; \beta)| \leq C_1$ and (D.1), we conclude

$$B_{(\beta, S, X)}(\widehat{\beta}^S; \beta) = \lim_{z \rightarrow 0^-} h_n(z) = \lim_{z \rightarrow 0^-} z^2 \beta^T \left(\frac{1}{p} X^T V^T V X - z I_p \right)^{-1} \Sigma \left(\frac{1}{p} X^T V^T V X - z I_p \right)^{-1} \beta.$$

Next, we follow the same idea as in the proof to the bias part in Theorem 3.2 to verify the interchange of the limits $n \rightarrow \infty$ and $z \rightarrow 0^-$. Since for any $z < 0$, $|h_n(z)| \leq C_1$ and

$$\begin{aligned} & |h'_n(z)| \\ & \leq 2 \|\Sigma\|_2 \|\beta\|^2 \left\| z \left(\frac{1}{p} X^T V^T V X - z I_p \right)^{-1} \right\|_2 \left\| \left(\frac{1}{p} X^T V^T V X - z I_p \right)^{-1} + z \left(\frac{1}{p} X^T V^T V X - z I_p \right)^{-2} \right\|_2 \\ & \leq \frac{\lambda_{\min}^+ \left(\frac{1}{p} X^T V^T V X \right) \|\Sigma\|_2}{\left[\lambda_{\min}^+ \left(\frac{1}{p} X^T V^T V X \right) - z \right]^2} \leq \frac{2C_1}{C_0 \tau}, \end{aligned}$$

where the second and the last inequalities follow (C.6) and hold almost surely for all large n , we can exchange limits by Arzela-Ascoli theorem and Moore-Osgood theorem, that is,

$$\lim_{n \rightarrow \infty} B_{(\beta, S, X)}(\widehat{\beta}^S; \beta) = \lim_{n \rightarrow \infty} \lim_{z \rightarrow 0^-} h_n(z) = \lim_{z \rightarrow 0^-} \lim_{n \rightarrow \infty} h_n(z). \tag{D.2}$$

Next, we aim to find $\lim_{z \rightarrow 0^-} \lim_{n \rightarrow \infty} h_n(z)$. Let $\mathbb{D} = \{(z, w) \in \mathbb{R}^2 : z < 0, w > -\frac{1}{2C_1}\}$,

$$\mathcal{H}_n(z, w) = z \beta^T \left(\frac{1}{p} X^T V^T V X - z I_p - z w \Sigma \right)^{-1} \beta$$

which is defined on \mathbb{D} , and

$$\Sigma_w = \Sigma \left(I_p + w\Sigma \right)^{-1}, \quad \beta_w = \left(I_p + w\Sigma \right)^{-1/2} \beta.$$

Then, $\mathcal{H}_n(z, w)$ is analytic on \mathbb{D} such that

$$\begin{aligned} \mathcal{H}_n(z, w) &= z\beta_w^T \left(\frac{1}{p} \Sigma_w^{1/2} Z^T V^T V Z \Sigma_w^{1/2} - z I_p \right)^{-1} \beta_w \\ h_n(z) &= \frac{\partial \mathcal{H}_n}{\partial w}(z, 0). \end{aligned}$$

Further write

$$m_{1n}(z, w) = \frac{1}{p} \text{tr} \left[\left(\frac{1}{p} \Sigma_w^{1/2} Z^T V^T V Z \Sigma_w^{1/2} - z I_p \right)^{-1} \Sigma_w \right], \quad m_{2n}(z, w) = \frac{1}{p} \text{tr} \left[\left(\frac{1}{p} V Z \Sigma_w Z^T V^T - z I_m \right)^{-1} \right].$$

According to (Paul & Silverstein, 2009) or (Couillet & Liao, 2022, Theorem 2.7), $-\frac{1}{z} \left(I_p + m_{2n}(z, w) \Sigma_w \right)^{-1}$ is the deterministic equivalent of $\left(\frac{1}{p} \Sigma_w^{1/2} Z^T V^T V Z \Sigma_w^{1/2} - z I_p \right)^{-1}$. Thus, it holds that, for any given $(z, w) \in \mathbb{D}$, as $n \rightarrow \infty$,

$$\mathcal{H}_n(z, w) - \tilde{\mathcal{H}}_n(z, w) \rightarrow 0 \quad \text{almost surely},$$

where $\tilde{\mathcal{H}}_n(z, w)$ is defined as

$$\tilde{\mathcal{H}}_n(z, w) = -\beta_w^T \left(I_p + m_{2n}(z, w) \Sigma_w \right)^{-1} \beta_w.$$

Furthermore, it is easy to show that $\mathcal{H}_n(z, w)$ and $\tilde{\mathcal{H}}_n(z, w)$ are both uniformly bounded on \mathbb{D} . Thus, using the Vitali's theorem collected as Lemma C.4, we have for $z < 0$

$$\begin{aligned} \lim_{n \rightarrow \infty} h_n(z) &= \lim_{n \rightarrow \infty} \frac{\partial \tilde{\mathcal{H}}_n}{\partial w}(z, 0) \\ &= \lim_{n \rightarrow \infty} \left(1 + \frac{\partial m_{2n}}{\partial w}(z, 0) \right) \beta^T [1 + m_{2n}(z, 0) \Sigma]^{-2} \Sigma \beta \\ &= \left(1 + \frac{\partial m_2}{\partial w}(z, 0) \right) \int \frac{x}{[1 + m_2(z, 0) x]^2} dG(x) \end{aligned} \quad (\text{D.3})$$

almost surely, where, according to (Zhang, 2007), $m_{1n}(z, w) \rightarrow m_1(z, w)$ and $m_{2n}(z, w) \rightarrow m_2(z, w)$ almost surely as $n \rightarrow \infty$. Moreover, for any given $(z, w) \in \mathbb{D}$, $(m_1(z, w), m_2(z, w)) \in \mathbb{R}^+ \times \mathbb{R}^+$ is the unique solution to the self-consistent equations

$$\begin{aligned} m_1(z, w) &= \int \frac{x}{-z [1 + wx + xm_2(z, w)]} dH(x), \\ m_2(z, w) &= \psi \phi^{-1} \frac{1}{-z [1 + m_1(z, w)]}. \end{aligned} \quad (\text{D.4})$$

Substituting m_2 into m_1 in (D.4) and using $m_1(z, 0) = m_1(z)$ as defined in (C.8), we have after some calculations

$$\lim_{z \rightarrow 0^-} z \frac{\partial m_1}{\partial w}(z, 0) = \frac{\int \frac{c_0^2 x^2}{(c_0 - x \psi \phi^{-1})^2} dH(x)}{1 - \int \frac{x^2 \psi \phi^{-1}}{(c_0 - x \psi \phi^{-1})^2} dH(x)} = \phi \psi^{-1} c_1 c_0^2.$$

where c_0 is defined in (4.1) and $\lim_{z \rightarrow 0^-} zm_1(z) = c_0$. Using (D.2) and continue (D.3), we have almost surely

$$\begin{aligned}
\lim_{n \rightarrow \infty} B_{(S,X)}(\widehat{\beta}^S; \beta) &= \lim_{z \rightarrow 0^-} \lim_{n \rightarrow \infty} h_n(z) \\
&= \lim_{z \rightarrow 0^-} \left(1 + \frac{\partial m_2}{\partial w}(z, 0) \right) \int \frac{x}{[1 + m_2(z, 0)x]^2} dG(x) \\
&= \lim_{z \rightarrow 0^-} \left(1 + \psi\phi^{-1} \frac{z \frac{\partial m_1}{\partial w}(z, 0)}{[z + zm_1(z)]^2} \right) \int \frac{x}{\left[1 - \psi\phi^{-1}x \frac{1}{z + zm_1(z)} \right]^2} dG(x) \\
&= (1 + c_1) \int \frac{c_0^2 x}{(c_0 - x\psi\phi^{-1})^2} dG(x).
\end{aligned}$$

E Proofs for central limit theorems

E.1 Proof of Theorem 6.4

For the underparameterized case with $\phi\psi^{-1} < 1$, by Lemma 3.1, it holds that

$$B_{(S,X)}(\widehat{\beta}^S; \beta) = 0, \quad V_{(S,X)}(\widehat{\beta}^S; \beta) = \sigma^2 \text{tr} \{(X^T S^T S X)^+\}.$$

Assume that $p < m < n$. Then $X^T S^T S X$ is of rank p and then invertible. So

$$\begin{aligned}
R_{(S,X)}(\widehat{\beta}^S; \beta) &= V_{(S,X)}(\widehat{\beta}^S; \beta) = \sigma^2 \text{tr} \{(X^T S^T S X)^{-1}\} = \frac{\sigma^2}{p} \text{tr} \{(X^T S^T S X/p)^{-1}\} \\
&= \sigma^2 \int \frac{1}{t} dF^{X^T S^T S X/p}(t) =: \sigma^2 s_{1n}(0),
\end{aligned}$$

where $s_{1n}(\cdot)$ denotes the Stieltjes transformation of the ESD $F^{X^T S^T S X/n}$ of $X^T S^T S X/n \in \mathbb{R}^{p \times p}$.

Let H_n denote the ESD of $S^T S \in \mathbb{R}^{n \times n}$ and H its LSD. Define

$$B_n := \frac{1}{p} (S^T S)^{1/2} X X^T (S^T S)^{1/2} \in \mathbb{R}^{n \times n}.$$

Under Assumptions 6.3, the matrix B_n has the LSD $F^{\phi^{-1}, H}$ which is the Marcehnko-Pastur law. Further, we define

$$G_n(t) := n \{ F^{B_n}(t) - F^{\phi^{-1}, H_n}(t) \}$$

where we use F^{ϕ^{-1}, H_n} instead of $F^{\phi^{-1}, H}$ to avoid discussing the convergence of (ϕ_n^{-1}, H_n) to (ϕ^{-1}, H) . For orthogonal sketching, $H_n = (1 - \psi_n)\delta_0 + \psi_n\delta_1$ and $H = (1 - \psi)\delta_0 + \psi\delta_1$. Notice that

$$G_n(t) = p \{ F^{X^T S^T S X/p}(t) - F^{\phi^{-1}, H_n}(t) \}$$

with $\underline{F}^{\phi_n^{-1}, H_n} := (1 - \phi_n^{-1})\delta_0 + \phi_n^{-1}F^{\phi_n^{-1}, H_n}$. By Theorem 3.2, we have

$$R_{(S,X)}(\widehat{\beta}^S, \beta) \xrightarrow{a.s.} \frac{\sigma^2 \phi \psi^{-1}}{1 - \phi \psi^{-1}}.$$

Further, we can rewrite

$$p\left(R_{(S,X)}(\widehat{\beta}^S, \beta) - \frac{\sigma^2 \phi_n \psi_n^{-1}}{1 - \phi_n \psi_n^{-1}}\right) = \sigma^2 \int \frac{1}{t} dG_n(t), \quad (\text{E.1})$$

where we replaced (ϕ, ψ) by (ϕ_n, ψ_n) when centering.

We prove the CLT for (E.1) in the following two steps.

Step 1. Given the sketching matrix S , by (Zheng et al., 2015, Theorem 2.1), the RHS of (E.1) converges to a Gaussian distribution with mean μ_1 and variance σ_1^2 specified as

$$\begin{aligned} \mu_1 = & -\frac{\sigma^2}{2\pi i} \oint_C \frac{1}{z} \frac{\phi^{-1} \int \underline{s}_\phi(z)^3 t^2 (1 + t \underline{s}_\phi(z))^{-3} dH(t)}{\left\{1 - \phi^{-1} \int \underline{s}_\phi^2 t^2 (1 + t \underline{s}_\phi(z))^{-2} dH(t)\right\}^2} dz \\ & - \frac{\sigma^2(\nu_4 - 3)}{2\pi i} \oint_C \frac{1}{z} \frac{\phi^{-1} \int \underline{s}_\phi(z)^3 t^2 (1 + t \underline{s}_\phi(z))^{-3} dH(t)}{1 - \phi^{-1} \int \underline{s}_\phi^2 t^2 (1 + t \underline{s}_\phi(z))^{-2} dH(t)} dz \end{aligned}$$

and

$$\begin{aligned} \sigma_1^2 = & -\frac{2\sigma^4}{4\pi^2} \oint_{C_1} \oint_{C_2} \frac{1}{z_1 z_2} \frac{1}{(\underline{s}_\phi(z_1) - \underline{s}_\phi(z_2))^2} d\underline{s}_\phi(z_1) d\underline{s}_\phi(z_2) \\ & - \frac{\phi^{-1}(\nu_4 - 3)}{4\pi^2} \oint_{C_1} \oint_{C_2} \frac{1}{z_1 z_2} \left\{ \int \frac{t}{(\underline{s}_\phi(z_1) + 1)^2} \frac{t}{(\underline{s}_\phi(z_2) + 1)^2} dH(t) \right\} d\underline{s}_\phi(z_1) d\underline{s}_\phi(z_2), \end{aligned}$$

where $\underline{s}_\phi(\cdot)$ denotes the Stieltjes transformation of $\underline{F}^{\phi^{-1}, H}$, and C, C_1 and C_2 are contours containing the support of the LSD of $\underline{s}_\phi(z)$.

Following the calculation of μ_c and σ_c^2 in the proof of (Li et al., 2021, Theorem 4.1), we get

$$\mu_1 = \frac{\sigma^2 \phi^2 \psi^{-2}}{(\phi \psi^{-1} - 1)^2} + \frac{\sigma^2 \phi^2 \psi^{-2} (\nu_4 - 3)}{1 - \phi \psi^{-1}}, \quad \sigma_1^2 = \frac{2\sigma^4 \phi^3 \psi^{-3}}{(\phi \psi^{-1} - 1)^4} + \frac{\phi^3 \psi^{-3} \sigma^4 (\nu_4 - 3)}{(1 - \phi \psi^{-1})^2}.$$

Step 2. Note that the mean μ_1 and variance σ_1^2 are nonrandom. It means that the limiting distribution of the RHS of (E.1) is independent of conditioning SS^\top . So it asymptotically follows the Gaussian distribution $\mathcal{N}(\mu_1, \sigma_1^2)$.

E.2 Proof of Theorem 6.5

For the overparameterized regime with $\phi \psi^{-1} > 1$, when $\Sigma = I_p$, we have

$$B_{(S,X)}(\widehat{\beta}^S, \beta) = \frac{\alpha^2}{p} \text{tr} \left\{ I_p - (X^\top S^\top S X)^+ X^\top S^\top S X \right\} = \alpha^2 - \frac{\alpha^2}{p} \text{tr} \left\{ (X^\top S^\top S X)^+ X^\top S^\top S X \right\}$$

$$= \alpha^2 - \frac{\alpha^2}{p} \text{tr} \{(SXX^T S^T)^+ SXX^T S^T\} = \alpha^2 (1 - \phi^{-1} \psi_n)$$

and

$$\begin{aligned} V_{(S,X)}(\widehat{\beta}^S; \beta) &= \sigma^2 \text{tr} \{(X^T S^T S X)^+\} = \sigma^2 \frac{1}{n} \text{tr} \{(SXX^T S^T/n)^{-1}\} \\ &= \sigma^2 \int \frac{1}{t} dF^{SXX^T S^T/n}(t) =: \sigma^2 \underline{s}_{1n}(0), \end{aligned}$$

where $\underline{s}_{1n}(z)$ denotes the Stieltjes transformation of the ESD $F^{SXX^T S^T/n}$ of $SXX^T S^T/n$ and it satisfies

$$\frac{p}{m} \underline{s}_{1n}(z) = -\frac{1}{z} \left(\frac{p}{m} - 1 \right) + \underline{s}_{1n}(z).$$

Following the proof of (Li et al., 2021, Theorem 4.3), we get

$$\mu_2 = \frac{\sigma^2 \phi \psi^{-1}}{(\phi \psi^{-1} - 1)^2} + \frac{\sigma^2 (\nu_4 - 3)}{\phi \psi^{-1} - 1}, \quad \sigma_2^2 = \frac{2\sigma^4 \phi^3 \psi^{-3}}{(\phi \psi^{-1} - 1)^4} + \frac{\sigma^4 \phi \psi^{-1} (\nu_4 - 3)}{(\phi \psi^{-1} - 1)^2}.$$

E.3 Proof of Theorem 6.7

Leveraging (Bai & Yao, 2008, Theorem 7.2) or following a similar proof to that of (Li et al., 2021, Theorem 4.5), we obtain

$$\begin{aligned} &\sqrt{p} \{B_{(\beta,S,X)}(\widehat{\beta}^S; \beta) - \alpha^2 (1 - \phi_n^{-1} \psi_n)\} \\ &= \sqrt{p} \{\beta^T [I_p - (X^T V^T V X)^+ X^T V^T V X] \beta - \alpha^2 (1 - \phi_n^{-1} \psi_n)\} \xrightarrow{D} \mathcal{N}(0, d^2 = d_1^2 + d_2^2), \end{aligned}$$

where

$$d_1^2 = w p^2 (\mathbb{E}(\beta_1^4) - \gamma^2), \quad d_2^2 = 2p^2(\theta - w)\gamma^2$$

and

$$\gamma = \mathbb{E}(\beta_1^2) = \frac{\alpha^2}{p}, \quad \theta = \lim_{p \rightarrow \infty} \frac{1}{p} \text{tr} \{I_p - (X^T S^T S X)^+ X^T S^T S X\} = 1 - \phi^{-1} \psi.$$

Here w is the limit of the average of squared diagonal elements of $[I_p - (X^T V^T V X)^+ X^T V^T V X]$, which will be canceled out in d^2 under the assumption that β is multivariate normal. After some simple calculation, we have $d^2 = 2(1 - \phi^{-1} \psi) \alpha^4$. Thus,

$$\sqrt{p} \{B_{(\beta,S,X)}(\widehat{\beta}^S; \beta) - \alpha^2 (1 - \phi_n^{-1} \psi_n)\} \xrightarrow{D} \mathcal{N}(0, 2(1 - \phi^{-1} \psi) \alpha^4). \quad (\text{E.2})$$

Moreover, we have proved in the Theorem 6.5 that

$$p \left(V_{(\beta,S,X)}(\widehat{\beta}^S; \beta) - \frac{\sigma^2}{\phi_n \psi_n^{-1} - 1} \right) \xrightarrow{D} \mathcal{N}(\mu_2, \sigma_2^2) \quad (\text{E.3})$$

where

$$\mu_2 = \frac{\sigma^2 \phi \psi^{-1}}{(\phi \psi^{-1} - 1)^2} + \frac{\sigma^2 (\nu_4 - 3)}{\phi \psi^{-1} - 1}, \quad \sigma_2^2 = \frac{2\sigma^4 \phi^3 \psi^{-3}}{(\phi \psi^{-1} - 1)^4} + \frac{\sigma^4 \phi \psi^{-1} (\nu_4 - 3)}{(\phi \psi^{-1} - 1)^2}.$$

Combining (E.2) and (E.3) completes the proof.